Sterile neutrinos produced near the electroweak scale: Mixing angles, MSW resonances, and production rates

Jun Wu,[1,*] Chiu Man Ho,[2,3,†] and Daniel Boyanovsky[1,‡]

[1]*Department of Physics and Astronomy, University of Pittsburgh, Pittsburgh, Pennsylvania 15260, USA*
[2]*Department of Physics, University of California, Berkeley, California 94720, USA*
[3]*Theoretical Physics Group, Lawrence Berkeley National Laboratory, Berkeley, California 94720, USA*
(Received 24 February 2009; published 13 November 2009)

We study the production of sterile neutrinos in the region $T \sim M_W$ in an extension beyond the standard model with the seesaw mass matrix originating in Yukawa couplings to Higgs-like scalars with masses and vev's of the order of the electroweak scale. Sterile neutrinos are produced by the decay of scalars and standard model vector bosons. We obtain the index of refraction, dispersion relations, mixing angles in the medium and production rates including those for right-handed sterile neutrinos, from the standard model and beyond the standard model self-energies. For $1 \lesssim M_W/T \lesssim 3$ we find narrow MSW resonances with $k \lesssim T$ for both left- and right-handed neutrinos even in absence of a lepton asymmetry in the (active) neutrino sector, as well as very low energy ($k/T \ll |\xi|$) narrow MSW resonances in the presence of a lepton asymmetry consistent with the bounds from Wilkinson Microwave Anisotropy Probe and Big Bang Nucleosynthesis. For small vacuum mixing angle, consistent with observational bounds, the absorptive part of the self-energies lead to a strong damping regime very near the resonances resulting in the *exact* degeneracy of the propagating modes with a concomitant breakdown of adiabaticity. We argue that cosmological expansion sweeps through the resonances, *resonant and nonresonant* sterile neutrino production results in a highly *nonthermal* distribution function enhanced at small momentum $k < T$, with potentially important consequences for their free-streaming length and transfer function at small scales.

I. INTRODUCTION

In the concordance ΛCDM standard cosmological model, the Universe today is composed approximately by 70% of a dark energy component responsible for the acceleration, about 25% of dark matter (DM) and about 5% of ordinary matter (baryons). In this scenario the DM component is cold and collisionless, and structure formation proceeds in a hierarchical "bottom-up" manner: small scales become nonlinear and collapse first and their merger and accretion lead to structures on larger scales [1]. This is a consequence of the fact that cold dark matter (CDM) particles feature negligible velocity dispersion leading to a power spectrum that favors small scales. In this hierarchical scenario dense clumps that survive the merger process form satellite galaxies. Numerical simulations of structure formation with CDM predict many orders of magnitude more DM subhaloes than observed low luminosity dwarf galaxies [2–7]. These simulations also yield a density profile that increases monotonically towards the center [3,7–11] $\rho(r) \sim r^{-\gamma}$, $\gamma = 1$ corresponds to the Navarro-Frenk-White profile, but steeper profiles with $\gamma \sim 1.2$ have been found recently in numerical simulations [7]. These density profiles accurately describe clusters of galaxies but

there has been recent observational evidence that seems to indicate a shallow cored profile instead of cusps in dwarf spheroidal galaxies which are deemed to be DM dominated [12–17]. This core vs cusp controversy is still being debated, and recent arguments suggest that the interpretation of the data is subject to assumptions and modelling [18]. Recently yet another discrepancy between the predictions of ΛCDM and observations has been revealed, the "emptiness of voids", possibly related to the overabundance problem [19].

Warm dark matter particles (WDM) were invoked [20–23] as possible solutions to the core vs cusps and the overabundance problems in satellite galaxies. WDM particles feature a nonvanishing velocity dispersion with a range in between CDM and hot dark matter leading to a free-streaming scale that cuts off power at small scales thereby smoothing out small scale structure. If the free-streaming scale of the WDM particles is smaller than the scale of galaxy clusters, the large scale structure properties are indistinguishable from those of CDM, but may affect structure at small scales [24], thereby providing an explanation of the smoother inner profiles and the fewer satellites. A small scale cutoff in the DM power spectrum may also explain the apparent smallness of galaxies at $z \sim 3$ found in Ref. [25].

Although the interpretation of cores in dSphs may be challenged by alternative explanations, and the missing satellite problem could be resolved by astrophysical

*juw31@pitt.edu
†cmho@berkeley.edu
‡boyan@pitt.edu

mechanisms such as complex ''gastrophysics,'' and recent simulations suggest that the dynamics of subhalos is not too different in WDM and CDM models [26], there is an intrinsic interest in studying alternatives to the standard CDM paradigm.

Any particle physics explanation of DM involves extensions beyond the standard model (SM), allowing quite generally, both CDM and WDM candidates.

Sterile neutrinos, namely, $SU(2)$ singlets, with masses in the ~keV range may be suitable WDM candidates [27–35] and may provide possible solutions to other astrophysical problems [31]. The main property that is relevant for structure formation of any DM candidate is its distribution function after decoupling [34,36] which depends on the production mechanism and the quantum kinetic evolution from production to decoupling. Sterile neutrinos may be produced by various different mechanisms [27–33], among them nonresonant mixing, or Dodelson-Widrow (DW) [27–29] has been invoked often. However, there seems to be some tension between the x ray [37] and the Lyman-α forest data [38,39] leading to the suggestion [40] that DW-produced sterile neutrinos cannot be the dominant WDM component.

A phenomenologically appealing extension of the SM with only one scale has been recently proposed [30,35,41]. In this model sterile neutrinos may be produced by the decay of a gauge-singlet scalar with a mass of the order of the electroweak scale [31–33,42]. In this scenario sterile neutrinos are produced and decouple at a temperature of the order of the mass or the scalar [32,33,43].

Recently [43] the quantum kinetics of production and decoupling of ~keV sterile neutrinos in these models was studied with the result that production via the decay of the gauge-singlet scalar leads to a nonthermal distribution function that favors small momentum. This result was combined with an analytic method to obtain the transfer function during matter domination recently introduced in Ref. [44]. This method reveals the influence of the distribution function of the decoupled particle upon the power spectrum and free-streaming length [45]. The results of Ref. [43] point out that sterile neutrinos produced via the decay of gauge-singlet scalars in the model advocated in Refs. [30–33,42,43] yield *smaller* free-streaming lengths and an *enhancement* of power at small scales as compared to those produced by the DW mechanism. Combining the results for the distribution function of sterile neutrinos produced via scalar decay with abundance and phase space constraints from dwarf spheroidal galaxies [34] yields a narrow window for the mass of sterile neutrinos [43]: $0.56 \text{ keV} \lesssim M_s \lesssim 1.33 \text{ keV}$. The robustness of this bound has been confirmed in Ref. [46], but there may be some tension with recent analysis of the Lyman-α forest with nonthermal populations [47], although the results in this reference relate mainly to resonant production.

Recent observations of the x-ray spectra from the Ursa Minor dwarf spheroidal galaxy with the *Suzako* satellite

[48] suggest that sterile neutrinos with masses in the keV range with mixing angles $\theta \sim 10^{-5}$ remain viable candidates as main dark matter constituents, a result that seems to be confirmed by those of Ref. [47].

Motivation and objectives: The clustering properties of dark matter candidates depend on the free-streaming length which determines the scale below which power is suppressed. When the DM particle of mass M_s has become nonrelativistic, the free-streaming length is approximately given by

$$\lambda_{\rm fs} \simeq [\langle p^2 \rangle / M_s^2 G \rho]^{1/2},$$

where ρ is the DM density and the average is with the distribution function of the decoupled DM particle. Distribution functions that favor small momenta lead to smaller free-streaming lengths and more power a small scales [43–45].

The study in Ref. [43] revealed that the *nonresonant* mechanism of sterile neutrino production by scalar decay advocated in Refs. [30,32,33,42] leads to a nonthermal distribution function that favors small momenta with important consequences for structure formation and remarkable differences with sterile neutrinos produced by the DW mechanism [27], whose distribution function is that of a thermal relic that decoupled while relativistic, but multiplied by an overall factor [27]. This overall factor in the DW distribution function *only* affects the abundance, but for a fixed DM density ρ the resulting free-streaming length is that of a neutrino of mass M_s decoupled at the sterile neutrino decoupling temperature. For a fixed mass and relic density the nonthermal distribution function from the production mechanism studied in Refs. [32,33,43] yields a *smaller* $\lambda_{\rm fs}$ and more power at small scales than in the DW mechanism without modifying the large scale power spectrum.

In the extension beyond the standard model (bsm) advocated in Refs. [30,32,33,42,43] sterile neutrinos *mix* with active neutrinos via a Yukawa coupling to the standard model Higgs [30] whose expectation value yields a seesaw mass matrix. The diagonalization of this seesaw mass matrix yields interaction vertices between vector bosons and the sterilelike neutrino. This is important because the distribution functions being a function of the energy, are necessarily associated with mass or energy eigenstates, *not* flavor eigenstates.

The study in Refs. [32,33,43] reveals that sterile neutrinos are produced and decouple at a temperature of the order of the mass of the scalar, which in the model of Refs. [30,32,33,42] is of the order of the Higgs mass.

At this temperature the charged and neutral vector bosons are present in the medium with large abundance, comparable to that of the scalar. *Their decay into the sterilelike neutrinos will therefore contribute to their total abundance and distribution function. This is one of the main observations in this article*. The coupling of the

charged and neutral vector bosons to the sterilelike neutrino is suppressed by the (small) mixing angle, but since the standard model couplings are much larger than the Yukawa couplings of the scalar to the sterile neutrino, the question is whether the decay of vector bosons may lead to a substantial contribution to the production rate of the sterilelike neutrinos. For $M_s \sim$ keV and the expectation value of the Higgs-like scalar in the range ~ 100 GeV the Yukawa coupling $Y \sim 10^{-8}$, the production rate via this process $\propto Y^2$, whereas the contribution from Z, W decay would be expected to be $\propto \alpha_w \sin^2(\theta)$, with θ the mixing angle. For $\theta \sim 10^{-5}$ [42,48] the production rate of sterilelike neutrinos via vector boson decay can be of the same order of *or larger than* that from scalar decay. This observation suggests that sterile neutrino production via the decay of *vector bosons* in the medium may be competitive with the production via scalar decay.

At high temperature and or density the mixing angle is modified by medium effects [49–55], therefore the first step towards understanding whether vector boson decay contributes to the production of sterilelike neutrinos is to obtain the in-medium correction to the mixing angles.

A more general aspect of sterile neutrino production via vector boson decay at $T \sim M_W$ is that both the index of refraction (real part of the self-energy) and the production rate determined by the absorptive part (imaginary part of the self-energy) are of $\mathcal{O}(G_F)$. This is in contrast to the usual situation at temperatures much smaller than the electroweak scale when the index of refraction is of $\mathcal{O}(G_F)$, but the absorptive part is of $\mathcal{O}(G_F^2)$.

Although the finite temperature and density corrections to the index of refraction have been obtained for $T \ll M_{W,Z}$ [53–55], to the best of our knowledge the study of the self-energy, the index of refraction (real part) and absorptive part (width) at $T \simeq M_{W,Z}$ has not been carried out.

To be sure, upon the diagonalization of the mass matrix, standard model interaction vertices with the sterilelike neutrino lead to production processes via both charged and neutral current interactions such as $\bar{l}l \rightarrow \bar{\nu}_1\nu_2$; $\bar{f}f \rightarrow \bar{\nu}_1\nu_2$ with charged leptons (l) or quarks (f) and $\nu_1 \sim \nu_a$; $\nu_2 \sim \nu_s$ (active and sterile, respectively) for small mixing angle. These processes are of $\mathcal{O}(\alpha_w^2 \sin^2\theta)$ and while they will eventually become important for $T \ll M_{W,Z}$ when the population of vector bosons in the medium becomes $\ll \alpha_w$, these are formally subleading in the weak coupling at $T \sim M_{W,Z}$.

Therefore at $T \sim M_{W,Z}$ vector boson decay is the *leading* production mechanism from weak interactions.

Our objective is to provide a comprehensive assessment of sterile neutrinos as potential DM candidates implementing the following program:

(i) Obtain the production rates and mixing angle in the medium from the quantum field theory model at $T \sim M_W$, studying the possibility of MSW resonances to determine whether sterile neutrinos are produced resonantly or nonresonantly.

(ii) Obtain and solve the kinetic equations describing the production and decoupling of sterile neutrinos using the rates and mixing angles obtained from previous step.

(iii) The asymptotic solution of the kinetic equation yields the distribution function after freeze-out, which determines the abundance and the free-streaming length. This distribution function is input in the program described in Refs. [43,44] to obtain the transfer function and power spectrum.

In this article we carry out the first step of this program. We implement methods of field theory at finite temperature and density developed in Refs. [54,56–59] to obtain the mixing angles in the medium and production rates both from scalar and vector boson decay.

Results: We study a simple extension of the standard model with one active and one sterile neutrino to extract the robust features in a simpler setting. Both active and sterile neutrinos are considered to be Dirac, this is to include the possibility of a lepton asymmetry hidden in the (active) neutrino sector (Majorana neutrinos cannot be assigned a chemical potential), and to allow us to study the production of left- and right-handed neutrinos.

We obtain the dispersion relations, index of refraction, mixing angles, and production rates in the medium from the self-energy contributions from standard model sm and bsm interactions. The seesaw mass matrix that mixes them emerges from the Yukawa couplings to Higgslike scalars with masses of the order of $M_{W,Z}$ that acquire expectation values also of this order. We focus on the temperature region $T \sim M_W$ where vector and scalar bosons are present in the medium with large thermal populations. The decay of both the scalar and vector bosons contribute to the production of sterile neutrinos. Our main results are:

(i) We find one MSW resonance even in the *absence* of a lepton asymmetry. For $1 \lesssim M_W/T \lesssim 3$ this resonance is in the low momentum region $0.2 \lesssim k/T \lesssim 1$ and well within the regime of validity of the perturbative expansion. Including a lepton asymmetry in the active neutrino sector consistent with the data from Wilkinson Microwave Anisotropy Probe (WMAP) and Big Bang Nucleosynthesis (BBN) [60], we find *two* low energy MSW resonances, the lowest one is a consequence of the lepton asymmetry that occurs at $k/T \ll \xi$ with $|\xi|$ being the lepton asymmetry parameter. In the region of interest for this study for small vacuum mixing angle consistent with the observational bounds from x-ray data [48] these resonances are very narrow. We find resonances also for positive energy, positive helicity, namely, nearly *right-handed* neutrinos.

(ii) At the resonances the propagating frequencies become exactly *degenerate* in striking contrast with the

quantum mechanics of neutrino mixing wherein there is level repulsion at the resonance. This exact degeneracy at the resonance entails the breakdown of adiabaticity. It is a distinct consequence of the absorptive part of the self-energy and leads to a strong damping regime.

(iii) The form of the standard model contribution to the production rate is similar to that from scalar decay found in Ref. [43]. We argue that cosmological expansion will lead to a rapid crossing of the narrow resonances resulting in both *resonant and nonresonant* sterile neutrino production. In particular nearly *right-handed* sterile neutrinos are produced by the decay of Z^0, $W^{\pm}$ vector bosons. Their distribution functions after freeze-out will be *highly nonthermal* with a distinct enhancement at small momentum $k < T$ and perturbatively small population. This low momentum enhancement of the nonthermal distribution function is expected [43,44] to have important consequences: a shortening of the free-streaming length (smaller velocity dispersion) and an increase of the transfer function and power spectrum at small scales.

(iv) We find a consistent range of parameters for which there is a resonance for positive helicity, positive energy neutrinos, namely, nearly right-handed at $T \sim M_W$. The general field theory framework allows a systematic study of the properties for both helicity states, including the helicity dependence of mixing angles and production rates.

II. THE MODEL

The extension of the standard model presented in Refs. [32,33,42] generalizes the proposal of the ν MSM of Refs. [30,41] and is also a generalization of the model presented in Ref. [61]. These models include three $SU(2)$ singlet (sterile) neutrinos which couple to the active neutrinos via a seesaw mass matrix. The generalization of Refs. [32,33,42] gives a mass to the sterile neutrino via a Yukawa coupling to a Higgslike scalar field which *could* be the neutral Higgs component, or another scalar whose expectation value is of the same order as that of the sm Higgs boson, therefore this type of extension features only one scale.

We study a simplified version of these models by considering only one sterile and one active neutrino. In the usual seesaw mechanism an off-diagonal Dirac mass matrix for the active species is considered along with a diagonal Majorana mass for the sterile neutrino [30,41,50–52]. However, instead of considering a Majorana sterile neutrino, we allow for Dirac mass terms for all species. This generalization allows to study simultaneously the possibility of a lepton asymmetry in the (active) neutrino sector for which a Dirac field is required, along with the possibility of a right-handed component

leading to potentially relevant degrees of freedom within the same simple model.

Our goal is to extract generic and robust features of the production rates and mixing angles in the medium along with a reliable estimate of sterile production rates. The generalization to three species can be done relatively straightforwardly (but for the complications associated with dealing with larger mixing matrices), and the case of a Majorana neutrino is regained straightforwardly by projection.

We consider a model with one active (ν_a) and one sterile (ν_s) (an $SU(2)$ singlet) Dirac neutrinos, described by the Lagrangian density

$$\mathcal{L} = \mathcal{L}_{SM} + \bar{\nu}_s i \not{\partial} \nu_s - Y_1 \bar{\nu}_s \tilde{H}^{\dagger} l - Y_2 \bar{\nu}_s \Phi \nu_s + \mathcal{L}[\Phi] + \text{H.c.}, \tag{2.1}$$

where

$$l = \begin{pmatrix} \nu_a \\ f \end{pmatrix}; \qquad \tilde{H} = \begin{pmatrix} H^0 \\ H^- \end{pmatrix}. \tag{2.2}$$

f is the charged lepton associated with ν_a and H^0, H^- are the components of the standard model Higgs doublet, and Φ is a real scalar singlet field whose expectation value gives a Dirac mass to the sterile neutrino. The Lagrangian density $\mathcal{L}[\Phi]$ describes the kinetic and potential terms of Φ.

In unitary gauge we write

$$H^0 = \langle H^0 \rangle + \sigma; \qquad \Phi = \langle \Phi \rangle + \varphi \tag{2.3}$$

and consistently with the single scale assumption of the ν MSM: $\langle H^0 \rangle \sim \langle \Phi \rangle$ are of the same order of magnitude (the weak scale) and that their masses are also of the same scale. In fact our analysis is quite general, and this assumption will only be invoked for a quantitative assessment. The Lagrangian density (2.1) becomes

$$\mathcal{L} = \mathcal{L}_{SM} + \bar{\nu}_s i \not{\partial} \nu_s - \bar{\nu}_{\alpha} \mathbb{M}_{\alpha\beta} \nu_{\beta} - Y_1 \bar{\nu}_s \sigma \nu_a - Y_2 \bar{\nu}_s \varphi \nu_s + \mathcal{L}[\langle \Phi \rangle + \varphi] + \text{H.c.};$$

$$\alpha, \beta = a, s, \tag{2.4}$$

where

$$\mathbb{M} = \begin{pmatrix} 0 & m \\ m & M_s \end{pmatrix}; \qquad m = Y_1 \langle H^0 \rangle; \qquad M_s = Y_2 \langle \Phi \rangle. \tag{2.5}$$

Introducing the "flavor" doublet (ν_a, ν_s) the diagonalization of the mass term $\mathbb{M}$ is achieved by a unitary transformation to the mass basis (ν_1, ν_2), namely,

$$\begin{pmatrix} \nu_a \\ \nu_s \end{pmatrix} = U(\theta) \begin{pmatrix} \nu_1 \\ \nu_2 \end{pmatrix}; \qquad U(\theta) = \begin{pmatrix} \cos(\theta) & \sin(\theta) \\ -\sin(\theta) & \cos(\theta) \end{pmatrix}, \tag{2.6}$$

where

$$\cos(2\theta) = \frac{M_s}{[M_s^2 + 4m^2]^{1/2}};$$

$$\sin(2\theta) = \frac{2m}{[M_s^2 + 4m^2]^{1/2}}. \tag{2.7}$$

In the mass basis

$$\mathbb{M}_m = U^{-1}(\theta); \qquad \mathbb{M}U(\theta) = \begin{pmatrix} M_1 & 0 \\ 0 & M_2 \end{pmatrix};$$

$$M_1 = \frac{1}{2}[M_s - [M_s^2 + 4m^2]^{1/2}]; \tag{2.8}$$

$$M_2 = \frac{1}{2}[M_s + [M_s^2 + 4m^2]^{1/2}].$$

We focus on a seesaw with $M_s \sim \text{keV} \gg m$ therefore

$$M_1 \simeq -\frac{m^2}{M_s}; \qquad M_2 \simeq M_s;$$

$$\sin(2\theta) \simeq \frac{2m}{M_s} \sim \left|\frac{M_1}{M_2}\right|^{1/2} \ll 1. \tag{2.9}$$

Taking $\langle H^0 \rangle \sim \langle \Phi \rangle$ the small mixing angle entails that $Y_1 \ll Y_2$ which results in self-energy corrections from the σ exchange are subleading as compared to those from the φ exchange. For example taking $\langle \Phi \rangle \sim \langle H^0 \rangle$, and for a $\sim \text{keV}$ sterile neutrino it follows that

$$Y_2 \sim 10^{-8} \gg Y_1; \qquad \sin(2\theta) \sim Y_1/Y_2. \tag{2.10}$$

However, we can alternatively consider a predetermined seesaw mass matrix and set $Y_1 = Y_2 = 0$ which corresponding to a simpler extension of the standard model that posits a mass matrix that originates beyond the standard model.

Our goal is to obtain the dynamical aspects of sterile neutrinos in the medium, mixing angles, dispersion relations, and damping rates, which determine the production rates. These are obtained directly from the solution of the equations of motion including the self-energy corrections in the medium. The one-loop self-energies require the neutrino *propagators* in the medium in the *mass basis*, since the mass eigenstates are the true propagating states. For $\theta \ll 1$ the mass eigenstates $\nu_1 \sim \nu_a$; $\nu_2 \sim \nu_s$, and the active neutrino reaches equilibrium at $T \gtrsim 1$ MeV via the weak interactions, whereas the sterile neutrinos are not expected to equilibrate.

This argument, however, hinges on the smallness of the vacuum mixing angle, but in a medium the mixing angle can become very large, and if there are MSW resonances the roles of the medium eigenstates may be reversed. Whether there are MSW resonances and the medium mixing angle becomes large can only be answered *a posteriori*.

Therefore we *assume* that the mass eigenstate ν_1 is activelike, and features a Fermi-Dirac distribution function, whereas for ν_2 the propagators are the vacuum ones. Furthermore, it is possible that if there is a large lepton asymmetry it may be stored in the neutrino sector, whereas

the asymmetry in the charged leptons equals the baryon asymmetry and can be neglected. Hence the Fermi-Dirac distribution functions in the ν_1 propagator includes a chemical potential.

In our study we explicitly separate the fermionic and bosonic contributions to the self-energies to assess the consistency of the assumption that the eigenstate "1" is activelike.

III. EQUATIONS OF MOTION

The effective Dirac equation in the medium is derived with the methods of nonequilibrium quantum field theory described in [56,57,59]. We follow the approach presented in Refs. [56,57] and introduce an external Grassmann-valued source that couples linearly to the neutrino field via the Lagrangian density

$$\mathcal{L}_S = \bar{\nu}_\alpha \eta_\alpha + \bar{\eta}_\alpha \nu_\alpha, \tag{3.1}$$

whence the total Lagrangian density is given by $\mathcal{L} + \mathcal{L}_S$. The external source induces an expectation value for the neutrino field which obeys the effective equation of motion with self-energy corrections from the medium [59].

The equation of motion is derived by shifting the field $\nu_\alpha^\pm = \psi_\alpha + \Psi_\alpha^\pm$, $\psi_\alpha = \langle \nu_\alpha^\pm \rangle$ imposing $\langle \Psi_\alpha^\pm \rangle = 0$ order by order in the perturbation theory [56,57,59]. Since the self-energy corrections to the equations of motion require the neutrino propagators, we obtain the equation of motion in the mass basis.

Implementing this program up to one-loop order, we find the following equation of motion for the doublet in the mass basis $\psi^T \equiv (\psi_1, \psi_2)$, it is given by

$$(i\slashed{\partial}\mathbb{1} - \mathbb{M}_m + \Sigma_{\text{sm}}^{\text{tad}}L)\psi(\vec{x}, t) + \int d^3x' dt'[\Sigma_{\text{sm}}^{\text{ret}}(\vec{x} - \vec{x}', t - t')L$$
$$+ \Sigma_{\text{bsm}}^{\text{ret}}(\vec{x} - \vec{x}', t - t')]\psi(\vec{x}', t') = -\eta(\vec{x}, t), \tag{3.2}$$

where $\mathbb{1}$ is the identity matrix, $\mathbb{M}_m = \text{diag}(M_1, M_2)$ is the mass matrix in the mass basis, $L = (1 - \gamma^5)/2$ is the left-handed chiral projection operator, $\Sigma_{\text{sm}}^{\text{tad}}$ is the (local) tadpole contribution from the sm neutral current interaction (see Fig. 1). $\Sigma_{\text{sm}}^{\text{ret}}(\vec{x} - \vec{x}', t - t')$ and $\Sigma_{\text{bsm}}^{\text{ret}}(\vec{x} - \vec{x}', t - t')$ are, respectively, the real-time retarded self-energies from sm and bsm (scalar) interactions. Introducing the space-time Fourier transform in a spatial volume V

$$\psi(\vec{x}, t) = \frac{1}{\sqrt{V}} \sum_{\vec{k}} \int dk_0 e^{i\vec{k}\cdot\vec{x}} e^{-ik_0 t} \tilde{\psi}(k_0, \vec{k}) \tag{3.3}$$

and similarly for the self-energy kernels and the source term, the equation of motion in the mass basis becomes

$$[(\gamma_0 k_0 - \vec{\gamma}\cdot\vec{k})\mathbb{1} - \mathbb{M}_m + \Sigma_{\text{sm}}^{\text{tad}}L + \Sigma_{\text{sm}}(k_0, \vec{k})L$$
$$+ \Sigma_{\text{bsm}}(k_0, \vec{k})]\tilde{\psi}(k_0, \vec{k}) = -\tilde{\eta}(k_0, \vec{k}). \tag{3.4}$$

The space-time Fourier transform of the retarded self-energies (not the tadpole) feature a dispersive representa-
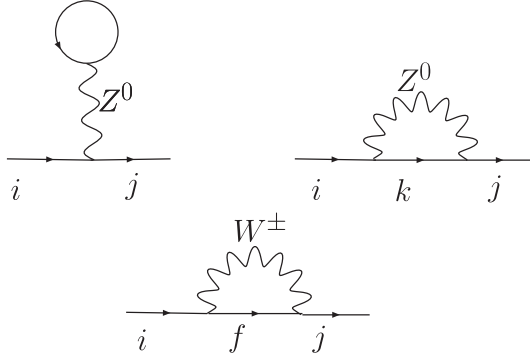
FIG. 1.   Standard model contributions to the self-energy Σ_{sm}. The indices i, k, $j = 1$, 2 corresponding to mass eigenstates, the index f for the intermediate fermion line in the charged-current self-energy refers to the charged lepton associated with the active neutrino.

tion

$$\Sigma(k_0, k) = \frac{1}{\pi} \int_{-\infty}^{\infty} d\omega \frac{\text{Im}\Sigma(\omega, \vec{k})}{\omega - k_0 - i0^+}. \quad (3.5)$$

A. One-loop self-energy

We focus on the temperature region $M_{Z,W,\sigma,\varphi} \gtrsim T$, in which using the unperturbed thermal propagators for the scalar and vector bosons is valid [62]. In Sec. V D we show that perturbation theory is valid for $k \gtrsim \alpha_w T$ or $M_{W,\sigma,\varphi} \gtrsim T$, furthermore for $k \ll M_W$ our results reproduce those found in the literature for $T \ll M_W$ [53,54], and the perturbative expansion is reliable for $M_W \gtrsim 2T$.

The sm charged and neutral current contributions to the self-energy in the mass basis are depicted in Fig. 1. The latin indices i, j, $k = 1$, 2 refer to the mass basis fields and the label f in the intermediate fermion propagator in the charged current diagram in Fig. 1 refers to the charged lepton associated with the active neutrino. The contributions from scalar exchange bsm in the mass basis are depicted in Fig. 2.

SM neutral currents: The tadpole contribution in the mass basis is given by

$$\Sigma_{\text{sm}}^{\text{tad}} = \Sigma^t U^{-1}(\theta) \begin{pmatrix} 1 & 0 \\ 0 & 0 \end{pmatrix} U(\theta), \quad (3.6)$$
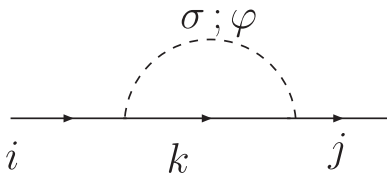
FIG. 2.   Beyond the standard model contributions to the self-energy Σ_{bsm}. The indices i, k, $j = 1$, 2 corresponding to mass eigenstates. The dashed line is a scalar propagator either for σ or φ.
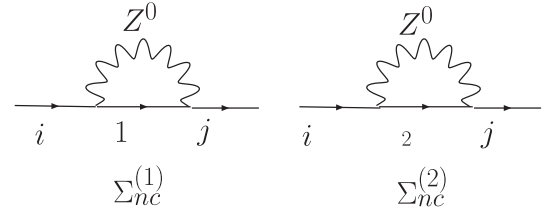
FIG. 3.   Neutral currents contribution to the one-loop retarded self-energy Σ_{sm}. The indices i, $j = 1$, 2 and the indices 1, 2 denote the corresponding mass eigenstate in the intermediate state.

where[1]

$$\Sigma^t = -\gamma^0 \frac{g^2}{4M_W^2} \int \frac{d^3q}{(2\pi)^3} (n_\nu - \bar{n}_\nu)$$

$$= -\gamma^0 \frac{g^2 T^3}{24M_W^2} \xi \left[1 + \frac{\xi^2}{\pi^2} \right];$$

$$\xi = \frac{\mu}{T}. \quad (3.7)$$

In this expression n_ν, $\bar{n}_\nu$ are the Fermi-Dirac distribution functions for neutrinos and antineutrinos, respectively, and we have neglected the contribution from the asymmetry of the charged lepton and quark sectors since these are proportional to the (negligible) baryon asymmetry. We allow for a lepton asymmetry stored in the neutrino sector. A recent analysis [60] from the latest WMAP and BBN data suggests that $|\xi| \lesssim 10^{-2}$.

The neutral current diagrams that contribute to the one-loop self-energy feature two different terms corresponding to the intermediate neutrino line being either ν_1 or ν_2. As argued above, for small mixing angles $\nu_1 \sim \nu_a$ and weak interactions equilibrate these mass eigenstates with the medium, therefore their finite temperature propagator features the Fermi-Dirac distribution function (with a chemical potential allowing for a lepton asymmetry). However, $\nu_2 \sim \nu_s$ will *not* equilibrate with the medium since their coupling to the environmental degrees of freedom is suppressed by at least two powers of the (small) mixing angle, therefore ν_2 features a vacuum propagator. The one-loop diagrams are shown in Fig. 3 where the superscripts (1) and (2) are used to specify the intermediate neutrino propagator ν_1 and ν_2 respectively.

In the mass basis we find for the neutral current contributions shown in Fig. 3

$$\Sigma_{nc}(k_0, \vec{k}) = [\cos^2(\theta)\Sigma_{nc}^{(1)}(k_0, \vec{k})$$

$$+ \sin^2(\theta)\Sigma_{nc}^{(2)}(k_0, \vec{k})]U^{-1}(\theta) \begin{pmatrix} 1 & 0 \\ 0 & 0 \end{pmatrix} U(\theta).$$

$$(3.8)$$

---

[1]This expression corrects a typographic error in Ref. [56].

sm charged currents: the charged current one-loop self-energy is shown in Fig. 1, since the intermediate state is a charged lepton we find in the mass basis

$$\Sigma_{cc}(k_0, \vec{k}) = \Sigma_{cc,\mathrm{sm}}(k_0, \vec{k}) U^{-1}(\theta) \begin{pmatrix} 1 & 0 \\ 0 & 0 \end{pmatrix} U(\theta), \quad (3.9)$$

where $\Sigma_{cc,\mathrm{sm}}(k_0, \vec{k})$ is the usual standard model one-loop self-energy in thermal equilibrium.

BSM scalar exchange: The scalar exchange contributions to the self-energy are shown in Fig. 4. For $\sin^2(\theta) \ll 1$ we find

$$\Sigma_{\mathrm{bsm}}(k_0, \vec{k}) = [\cos^2(\theta)\Sigma_\sigma^{(1)}(k_0, \vec{k}) + \sin^2(\theta)\Sigma_\varphi^{(1)}(k_0, \vec{k})$$
$$+ \cos^2(\theta)\Sigma_\varphi^{(2)}(k_0, \vec{k})]U^{-1}(\theta)\begin{pmatrix} 0 & 0 \\ 0 & 1 \end{pmatrix}U(\theta)$$
$$+ \cos^2(\theta)\Sigma_\varphi^{(2)}(k_0, \vec{k})U^{-1}(\theta)\begin{pmatrix} 1 & 0 \\ 0 & 0 \end{pmatrix}U(\theta).$$
$$(3.10)$$

Summary of self-energies in the flavor basis: The structure of the self-energies [to leading order in $\sin^2(\theta)$ (3.6), (3.7), (3.8), (3.9), and (3.10)] indicates that they are diagonal in the *flavor basis*. In this basis the total self-energy is given by

$$\Sigma(k_0, \vec{k}) = \begin{pmatrix} \Sigma_{aa}(k_0, \vec{k}) & 0 \\ 0 & \Sigma_{ss}(k_0, \vec{k}) \end{pmatrix}, \quad (3.11)$$

where

$$\Sigma_{aa}(k_0, \vec{k}) = [\Sigma^t + \cos^2(\theta)\Sigma_{nc}^{(1)}(k_0, \vec{k}) + \sin^2(\theta)\Sigma_{nc}^{(2)}(k_0, \vec{k})$$
$$+ \Sigma_{cc,\mathrm{sm}}(k_0, \vec{k})]L + \cos^2(\theta)\Sigma_\sigma^{(2)}(k_0, \vec{k}),$$
$$(3.12)$$

$$\Sigma_{ss}(k_0, k) = \cos^2(\theta)\Sigma_\sigma^{(1)}(k_0, \vec{k}) + \sin^2(\theta)\Sigma_\varphi^{(1)}(k_0, \vec{k})$$
$$+ \cos^2(\theta)\Sigma_\varphi^{(2)}(k_0, \vec{k}). \quad (3.13)$$

Since in the sm contributions we have explicitly factored out the left-handed projector L, the remainder contribu-
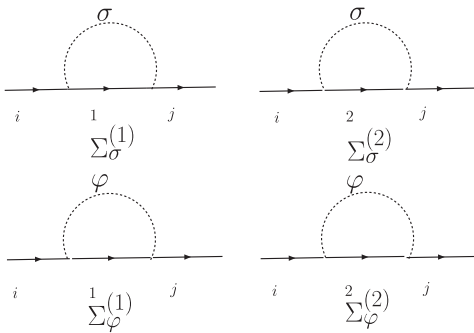
FIG. 4. Scalar exchange contributions to the one-loop self-energy Σ_{bsm}. The indices $i, j = 1, 2$ and the indices 1, 2 denote the corresponding mass eigenstate in the intermediate state.

tions to the sm self-energies $\Sigma_{nc,cc}$ are those of a vectorlike theory. The bsm contributions feature both chiralities since we have considered a Dirac mass term for the sterile neutrino, a left-handed Majorana mass term can be obtained by neglecting the right-handed contribution. We consider the regime $T \gg M_{1,2}, m_f$ and $k_0, k \gg M_{1,2}, m_f$, where m_f stand for the charged lepton masses; therefore, we can safely neglect the mass terms and consider the propagators of massless fermionic fields.

In this regime the general form of the sm self-energies with vector boson exchange, either charged or neutral currents is written in dispersive form as in Eq. (3.5) with [56,57]

$$\mathrm{Im}\Sigma_{\mathrm{sm}}(\omega, \vec{k}) = \pi g_{\mathrm{sm}}^2 \int \frac{d^3q}{(2\pi)^3} \int dp_0 dq_0 \delta(\omega - p_0 - q_0)$$
$$\times [1 - n_F(p_0) + N_B(q_0)]\gamma^\mu \rho_F(p_0, \vec{p})$$
$$\times \rho_B(q_0, \vec{q})\gamma^\nu P_{\mu\nu}(q_0, \vec{q}), \quad (3.14)$$

where F stands for the fermionic species in the intermediate state. For ν_1 and charged lepton n_F is the Fermi-Dirac distribution function, whereas for ν_2 it is $n_F = 0$ since the "sterile" neutrino does not thermalize with the medium. For the bsm contributions, the general form for scalar exchange is

$$\mathrm{Im}\Sigma_{\mathrm{bsm}}(\omega, \vec{k}) = \pi Y^2 \int \frac{d^3q}{(2\pi)^3} \int dp_0 dq_0 \delta(\omega - p_0 - q_0)$$
$$\times [1 - n_F(p_0) + N_B(q_0)]$$
$$\times \rho_F(p_0, \vec{p})\rho_B(q_0, \vec{q}) \quad (3.15)$$

where

$$g_{\mathrm{sm}} = \begin{cases} \frac{g}{\sqrt{2}} & \mathrm{CC} \\ \frac{g}{2\cos(\theta_w)} & \mathrm{NC} \end{cases} \quad (3.16)$$

and $Y = Y_1, Y_2$ for σ and φ exchange, respectively. The spectral densities are, respectively, (for massless fermions)

$$\rho_F(p_0, \vec{p}) = \frac{1}{2}\left(\gamma^0 - \vec{\gamma} \cdot \frac{\vec{p}}{p}\right)\delta(p_0 - p)$$
$$+ \frac{1}{2}\left(\gamma^0 + \vec{\gamma} \cdot \frac{\vec{p}}{p}\right)\delta(p_0 + p), \quad (3.17)$$

$$\rho_B(q_0, \vec{q}) = \frac{1}{2W_q}[\delta(q_0 - W_q) - \delta(q_0 + W_q)];$$

$$W_q = \sqrt{q^2 + M^2}. \quad (3.18)$$

The projection operator

$$P_{\mu\nu}(q_0, \vec{q}) = -\left[g_{\mu\nu} - \frac{q_\mu q_\nu}{M_{Z,W}^2}\right]; \qquad q^\mu = (q^0, \vec{q})$$

$$(3.19)$$

and

$$n_F(p_0) = \frac{1}{e^{(p_0 - \mu)/T} + 1};$$

$$\bar{n}_F(p_0) = 1 - n_\nu(-p_0); \tag{3.20}$$

$$N_B(q_0) = \frac{1}{e^{q_0/T} - 1}.$$

We have allowed a chemical potential for the neutrinos (only for $\nu_1 \sim \nu_a$) to include the possibility of a lepton asymmetry in the (active) neutrino sector.

In the expressions above, the masses for the scalars or vector bosons are $M_{\sigma,\varphi}$, $M_{Z,W}$ as appropriate for each contribution. All the self-energies share the general form

$$\Sigma(k_0, \vec{k}) \equiv \gamma^0 A(k_0, k) - \vec{\gamma} \cdot \hat{\mathbf{k}} B(k_0, k), \tag{3.21}$$

the detailed expressions for the imaginary parts of the sm and BSM contributions are given in the appendices.

In particular, for the neutral current tadpole $B(k_0, k) = 0$ and $A(k_0, k)$ can be recognized from Eq. (3.7). Combining (3.11) with this form we write the self-energy matrix in the *flavor basis* as

$$\Sigma_{\text{sm}}^{\text{tad}} L + \Sigma_{\text{sm}}(k_0, \vec{k}) L + \Sigma_{\text{bsm}}(k_0, \vec{k})$$
$$\equiv [\gamma^0 \mathbb{A}_L(k_0, k) - \vec{\gamma} \cdot \hat{\mathbf{k}} \mathbb{B}_L(k_0, k)] L$$
$$+ [\gamma^0 \mathbb{A}_R(k_0, k) - \vec{\gamma} . \hat{\mathbf{k}} \mathbb{B}_R(k_0, k)] R. \tag{3.22}$$

In the flavor basis these matrices are of the form

$$\mathbb{A}(k_0, k) = \begin{pmatrix} A_{aa}(k_0, k) & 0 \\ 0 & A_{ss}(k_0, k) \end{pmatrix};$$
$$\mathbb{B}(k_0, k) = \begin{pmatrix} B_{aa}(k_0, k) & 0 \\ 0 & B_{ss}(k_0, k) \end{pmatrix}, \tag{3.23}$$

where the matrix elements are obtained from the expressions (3.12) and (3.13).

The equations of motion for the left-handed (L) and right-handed (R) components are obtained by multiplying the equation of motion (3.4) on the left by the projectors R and L, respectively.

It proves convenient at this stage to separate the Dirac spinors into the left-handed ψ_L and right-handed ψ_R components and to expand them into helicity eigenstates [56], namely,

$$\psi_L = \sum_{h=\pm 1} v^h \otimes \varphi^h; \qquad \varphi^h = \begin{pmatrix} \varphi_a^h \\ \varphi_s^h \end{pmatrix}, \tag{3.24}$$

and

$$\psi_R = \sum_{h=\pm 1} v^h \otimes \zeta^h; \qquad \zeta^h = \begin{pmatrix} \zeta_a^h \\ \zeta_s^h \end{pmatrix}, \tag{3.25}$$

where the left-handed φ and right-handed ζ doublets are written in the *flavor* basis, and v^h are eigenstates of the helicity operator

$$\hat{h}(\hat{\mathbf{k}}) = \gamma^0 \vec{\gamma} \cdot \hat{\mathbf{k}} \gamma^5 = \vec{\sigma} \cdot \hat{\mathbf{k}} \begin{pmatrix} \mathbb{1} & 0 \\ 0 & \mathbb{1} \end{pmatrix}, \tag{3.26}$$

namely,

$$\vec{\sigma} \cdot \hat{\mathbf{k}} v^h = h v^h; \qquad h = \pm 1. \tag{3.27}$$

To leading order in weak and Yukawa couplings, and neglecting a commutator $[\mathbb{M}, \Sigma]$ because it is higher order in these couplings, we find in the *flavor* basis for both the left- and right-handed component doublets

$$\Big[(k_0^2 - k^2) \mathbb{1} + (k_0 - hk)(\mathbb{A}_L + h\mathbb{B}_L)$$
$$+ (k_0 + hk)(\mathbb{A}_R - h\mathbb{B}_R) - \mathbb{M}^2 \Big] \begin{Bmatrix} \varphi^h \\ \zeta^h \end{Bmatrix} = \begin{Bmatrix} I_L^h \\ I_R^h \end{Bmatrix}, \tag{3.28}$$

where $\mathbb{M}$ is the mass matrix in the *flavor* basis and the inhomogeneities in these equations are obtained by projection and using the corresponding equations, we need not specify them as they are no longer used in our study.

In absence of interactions, for the left-handed component a positive energy solution corresponds to $h = -1$ and a negative energy solution to $h = +1$ with the opposite assignment for the right-handed component.

In the flavor basis

$$\mathbb{M}^2 = \bar{M}^2 \mathbb{1} + \frac{\delta M^2}{2} \begin{pmatrix} -\cos(2\theta) & \sin(2\theta) \\ \sin(2\theta) & \cos(2\theta) \end{pmatrix}. \tag{3.29}$$

where

$$\bar{M}^2 \equiv \tfrac{1}{2}(M_1^2 + M_2^2); \qquad \delta M^2 \equiv M_2^2 - M_1^2, \tag{3.30}$$

and $M_{1,2}$ are given by Eq. (2.8).

It proves convenient to define the combinations

$$S_h(k_0, k) = (k_0 + hk)[\mathbb{A}_R - h\mathbb{B}_R)_{aa} + (\mathbb{A}_R - h\mathbb{B}_R)_{ss}]$$
$$+ (k_0 - hk)[(\mathbb{A}_L + h\mathbb{B}_L)_{aa} + (\mathbb{A}_L + h\mathbb{B}_L)_{ss}], \tag{3.31}$$

and

$$\Delta_h(k_0, k) = \frac{(k_0 + hk)}{\delta M^2} [(\mathbb{A}_R - h\mathbb{B}_R)_{aa} - (\mathbb{A}_R - h\mathbb{B}_R)_{ss}]$$
$$+ \frac{(k_0 - hk)}{\delta M^2} [(\mathbb{A}_L + h\mathbb{B}_L)_{aa} - (\mathbb{A}_L + h\mathbb{B}_L)_{ss}], \tag{3.32}$$

where we have suppressed the arguments. The equation of motion (3.28) can now be written as

$$\mathbb{G}_h^{-1}(k_0, k) \begin{Bmatrix} \varphi^h \\ \zeta^h \end{Bmatrix} = \begin{Bmatrix} I_L^h \\ I_R^h \end{Bmatrix}, \tag{3.33}$$

where the inverse propagator is given by

$$\mathbb{G}_h^{-1}(k_0, k) = \left(k_0^2 - k^2 + \frac{1}{2} S_h(k_0, k) - \bar{M}^2\right)\mathbb{I}$$

$$- \frac{1}{2}\delta M^2 \rho_h(k_0, k)$$

$$\times \begin{pmatrix} -C_h(k_0, k) & D_h(k_0, k) \\ D_h(k_0, k) & C_h(k_0, k) \end{pmatrix}, \qquad (3.34)$$

where

$$\rho_h(k_0, k) = [(\cos(2\theta) + \Delta_h(k_0, k))^2 + \sin^2(2\theta)]^{1/2} \qquad (3.35)$$

and

$$C_h(k_0, k) = \frac{(\cos(2\theta) + \Delta_h(k_0, k))}{\rho_h(k_0, k)}, \qquad (3.36)$$

$$D_h(k_0, k) = \frac{\sin(2\theta)}{\rho_h(k_0, k)}. \qquad (3.37)$$

We note that *if* $\Delta_h(k_0, k)$ were real, then $C_h(k_0, k) = \cos(2\theta_m^h(k_0, k))$ and $D_h(k_0, k) = \sin(2\theta_m^h(k_0, k))$ with $\theta_m^h(k_0, k)$ the mixing angle in the medium for the different helicity projections and as a function of frequency and momentum.

B. Propagator: complex poles and propagating modes in the medium

From (3.34) we read off the propagator projected onto helicity eigenstates

$$\mathbb{G}_h(k_0, k) = \frac{\mathbb{I} + \mathbb{T}_h(k_0, k)}{2(\alpha_h(k_0, k) - \beta_h(k_0, k))}$$

$$+ \frac{\mathbb{I} + \mathbb{T}_h(k_0, k)}{2(\alpha_h(k_0, k) + \beta_h(k_0, k))}, \qquad (3.38)$$

where

$$\mathbb{T}_h(k_0, k) = \begin{pmatrix} -C_h(k_0, k) & D_h(k_0, k) \\ D_h(k_0, k) & C_h(k_0, k) \end{pmatrix}, \qquad (3.39)$$

$$\alpha_h(k_0, k) = k_0^2 - k^2 + \tfrac{1}{2}S_h(k_0, k) - \bar{M}^2, \qquad (3.40)$$

$$\beta_h(k_0, k) = \tfrac{1}{2}\delta M^2 \rho_h(k_0, k). \qquad (3.41)$$

If $\Delta_h(k_0, k)$ given by Eq. (3.32) *were* real, the propagator (3.38) would be diagonalized by the unitary transformation

$$U_h(\theta_m^h(k_0, k)) = \begin{pmatrix} \cos(\theta_m^h(k_0, k)) & \sin(\theta_m^h(k_0, k)) \\ -\sin(\theta_m^h(k_0, k)) & \cos(\theta_m^h(k_0, k)) \end{pmatrix}, \qquad (3.42)$$

leading to

$$U^{-1}(\theta_m)\mathbb{G}(k_0, k)U(\theta_m) = \begin{pmatrix} \frac{1}{\alpha(k_0, k) + \beta(k_0, k)} & 0 \\ 0 & \frac{1}{\alpha(k_0, k) - \beta(k_0, k)} \end{pmatrix}, \qquad (3.43)$$

where we have suppressed the helicity argument for simplicity. However, because $\Delta_h(k_0, k)$ features an imaginary part determined by the absorptive part of the self-energies, there is no unitary transformation that diagonalizes the propagator. However, since the imaginary part is perturbatively small the expression (3.43) clearly indicates that the pole for $\alpha = \beta$ corresponds to the mass eigenstate 2, namely, a sterilelike neutrino state, and the pole for $\alpha = -\beta$ corresponds to the mass eigenstate 1, namely, an activelike state.

We note that in absence of interactions, namely, $S_h = 0$; $\Delta_h = 0$ it follows that

$$\alpha + \beta = k_0^2 - k^2 - M_1^2, \qquad (3.44)$$

$$\alpha - \beta = k_0^2 - k^2 - M_2^2. \qquad (3.45)$$

The propagating eigenstates in the medium are determined by the (complex) poles of the propagator (3.38), which again correspond to $\alpha_h(k_0, k) = \pm\beta_h(k_0, k)$.

Before we analyze the complex poles, it proves convenient to separate the real and imaginary parts of α, β. For this purpose and to simplify notation, we suppress the label h and the arguments k_0, k in these quantities, and we write

$$S = S_R + iS_I; \qquad \Delta = \Delta_R + i\Delta_I, \qquad (3.46)$$

where the subscripts R, I stand for real and imaginary parts, respectively. Furthermore, we *define* the mixing angles in the medium solely in terms of the *real* parts of the self-energy (index of refraction), namely,

$$\cos(2\theta_m) = \frac{\cos(2\theta) + \Delta_R}{\rho_0}; \qquad \sin(2\theta_m) = \frac{\sin(2\theta)}{\rho_0}, \qquad (3.47)$$

where

$$\rho_0 = [(\cos(2\theta) + \Delta_R)^2 + \sin^2(2\theta)]^{1/2}. \qquad (3.48)$$

An MSW resonance occurs whenever $\cos(2\theta_m) = 0$ [49–52], namely, when

$$\Delta_R = -\cos(2\theta). \qquad (3.49)$$

We emphasize that the mixing angle in the medium θ_m and ρ_0 depend on *helicity*, k_0, k. In terms of these quantities we find

$$\beta = \frac{\delta M^2}{2}\rho_0 r[\cos(\phi) + i\sin(\phi)] \equiv \beta_R + i\beta_I, \qquad (3.50)$$

where

$$r = [(1 - \tilde{\gamma}^2)^2 + (2\tilde{\gamma}\cos(2\theta_m))^2]^{1/4}; \qquad \tilde{\gamma} = \frac{\Delta_I}{\rho_0}, \qquad (3.51)$$

and

$$\phi = \text{sign}(\tilde{\gamma}\cos(2\theta_m))\Big\{\frac{1}{2}\text{arctg}\left|\frac{2\tilde{\gamma}\cos(2\theta_m)}{1 - \tilde{\gamma}^2}\right|\Theta(1 - \tilde{\gamma}^2)$$
$$+ \left(\frac{\pi}{2} - \frac{1}{2}\text{arctg}\left|\frac{2\tilde{\gamma}\cos(2\theta_m)}{1 - \tilde{\gamma}^2}\right|\right)\Theta(\tilde{\gamma}^2 - 1)\Big\}. \tag{3.52}$$

This form is similar to that obtained in a model of oscillations and damping with mixed neutrinos studied in Ref. [63], and suggests two distinct situations: a *weak damping* case for $|\tilde{\gamma}| < 1$ and a *strong damping* case for $|\tilde{\gamma}| > 1$. These cases will be analyzed below.

Zeroes of $\alpha + \beta$: We are concerned with the ultrarelativistic limit $k \gg M_2^2 \gg M_1^2$. Just as in the usual case [50–52] it is convenient to introduce the average or reference frequency

$$\bar{\omega}(k) = \sqrt{k^2 + \bar{M}^2}. \tag{3.53}$$

The poles are near $\bar{\omega}(k)$, therefore write

$$k_0 = \bar{\omega}(k) + (k_0 - \bar{\omega}(k)), \tag{3.54}$$

keeping only the linear term in $(k_0 - \bar{\omega}(k))$ we find

$$\alpha + \beta \sim 2\bar{\omega}(k)[k_0 - \Omega_1(k) + i\Gamma_1(k)] \tag{3.55}$$

with

$$\Omega_1(k) = \bar{\omega}(k) - \frac{1}{4\bar{\omega}(k)}[S_R + \delta M^2 \rho_0 r \cos(\phi)]_{k_0=\bar{\omega}(k)}, \tag{3.56}$$

$$\Gamma_1(k) = \frac{1}{4\bar{\omega}(k)}[S_I + \delta M^2 \rho_0 r \sin(\phi)]_{k_0=\bar{\omega}(k)}. \tag{3.57}$$

Zeroes of $\alpha - \beta$: Proceeding in the same manner, we find

$$\alpha - \beta \sim 2\bar{\omega}(k)[k_0 - \Omega_2(k) + i\Gamma_2(k)] \tag{3.58}$$

with

$$\Omega_2(k) = \bar{\omega}(k) - \frac{1}{4\bar{\omega}(k)}[S_R - \delta M^2 \rho_0 r \cos(\phi)]_{k_0=\bar{\omega}(k)}, \tag{3.59}$$

$$\Gamma_2(k) = \frac{1}{4\bar{\omega}(k)}[S_I - \delta M^2 \rho_0 r \sin(\phi)]_{k_0=\bar{\omega}(k)}. \tag{3.60}$$

From (3.55) and (3.58) it is clear that the propagator in the medium features two Breit-Wigner complex poles corresponding to the two propagating modes in the medium.

In the expressions above we have only focused on the positive energy modes. The expressions for the negative energy modes may be obtained from the following relations which are consequences of the imaginary parts of the self-energies and the dispersive representation valid both for scalar and vector boson exchange (3.5),

$$\text{Im}\,\mathbb{A}(-k_0, k; \mu) = \text{Im}\,\mathbb{A}(k_0, k; -\mu);$$
$$\text{Re}\,\mathbb{A}(-k_0, k; \mu) = -\text{Re}\,\mathbb{A}(k_0, k; -\mu), \tag{3.61}$$

$$\text{Im}\,\mathbb{B}(-k_0, k; \mu) = -\text{Im}\,\mathbb{B}(k_0, k; -\mu);$$
$$\text{Re}\,\mathbb{B}(-k_0, k; \mu) = \text{Re}\,\mathbb{B}(k_0, k; -\mu). \tag{3.62}$$

These properties can be read off the explicit expressions for the imaginary parts of the self-energies given in the Appendix Eqs. (A1)–(A3) for the standard model contributions and Eqs. (B1)–(B3) for the scalar exchange contributions. The matrices $\mathbb{A}$ are extracted from the coefficient of γ^0 and $\mathbb{B}$ from the coefficients of $\vec{\gamma} \cdot \hat{k}$ in the self-energies, respectively. The relations for the real parts follow from the dispersive representation (3.5).

In what follows we use the ultrarelativistic approximation

$$\bar{\omega}(k) \simeq k + \frac{\bar{M}^2}{2k}. \tag{3.63}$$

In the limit of interest $k/T \lesssim 1$ with $M_1 \ll M_2 \sim M_s \sim \mathcal{O}$ (keV), the region $k < T \sim \mathcal{O}(100 \text{ GeV})$ corresponds to a wide window in which the ultrarelativistic approximation is reliable.

We note that the difference in the real part of the pole position in the ultrarelativistic limit becomes

$$\Omega_2(k) - \Omega_1(k) \simeq \frac{\delta M^2}{2k}\rho_0 r \cos(\phi). \tag{3.64}$$

From the expression (3.52) for $|\tilde{\gamma}| > 1$ it follows that when an MSW resonance occurs, namely, for $\theta_m = \pi/4$ resulting in $\cos(\phi) = 0$ and the real part of the poles become *degenerate*. This is in striking contrast with the quantum mechanical description of mixed neutrinos where no level crossing (or complete degeneracy) can occur. Indeed the degeneracy is a consequence of the fact that the self-energy is complex and only occurs when damping is strong in the sense that $|\tilde{\gamma}| > 1$.

The degeneracy near an MSW resonance for strong damping will necessarily result in a breakdown of adiabaticity during cosmological evolution. We analyze below the conditions required for this phenomenon to occur.

Furthermore, as discussed in Refs. [32,43] decoupling and freeze-out of sterile neutrinos of neutrinos produced via scalar decay occurs near the electroweak scale, and it will be seen consistently that vector boson decay yields a production rate with a similar structure as for scalar decay therefore a similar range of temperatures in which sterile neutrino production by this mechanism is effective.

Perturbation theory is reliable when the change in the dispersion relations (positions of the poles in the propagators) is small. In the relativistic limit the (bare) poles correspond to $k_0 = k$ (for positive energy particles), therefore perturbation theory is valid for $k \gg (\Omega_{1,2} - k)$; $\Gamma_{1,2}$, namely, $k \gg \Sigma(k, k)$ where Σ is any of the self-energies. In

the next section we obtain explicitly the self-energies and in Sec. V D we assess the regime of validity of the perturbative expansion.

C. Helicity dependence: right-handed sterile neutrinos and standard model interactions

We have purposely kept the general form of the self-energies and propagators in terms of the helicity projections $h = \pm 1$. In the noninteracting massless case, positive energy left-handed particles correspond to $h = -1$ and negative energy left-handed correspond to $h = 1$, with the opposite assignment for right-handed particles. For the massive but ultrarelativistic case the mass term yields corrections to the handedness-helicity assignment of $\mathcal{O}(M^2/k^2)$.

$h = -1$: Neglecting subleading terms of $\mathcal{O}(\bar{M}^2/k^2)$ that multiply bsm right-handed contributions in the ultrarelativistic limit, we obtain

$$S(k) = 2k[(\mathbb{A}_L - \mathbb{B}_L)_{aa} + (\mathbb{A}_L - \mathbb{B}_L)_{ss}], \qquad (3.65)$$

$$\Delta(k) = \frac{2k}{\delta M^2}[(\mathbb{A}_L - \mathbb{B}_L)_{aa} - (\mathbb{A}_L - \mathbb{B}_L)_{ss}]. \qquad (3.66)$$

$h = 1$: In this case the corrections of $\mathcal{O}(\bar{M}^2/k^2)$ multiply sm left-handed contributions, which may be of the same order of the bsm right-handed contributions. We find

$$S(k) = 2k[(\mathbb{A}_R - \mathbb{B}_R)_{aa} + (\mathbb{A}_R - \mathbb{B}_R)_{ss}$$
$$+ \frac{\bar{M}^2}{4k^2}(\mathbb{A}_L + \mathbb{B}_L)_{aa}], \qquad (3.67)$$

$$\Delta(k) = \frac{2k}{\delta M^2}[(\mathbb{A}_R - \mathbb{B}_R)_{aa} - (\mathbb{A}_R - \mathbb{B}_R)_{ss}$$
$$+ \frac{\bar{M}^2}{4k^2}(\mathbb{A}_L + \mathbb{B}_L)_{aa}]. \qquad (3.68)$$

The terms proportional to $\bar{M}^2/4k^2$ only receive contribution from the *standard model* self-energies, whereas the right-handed components only originate in the contributions beyond the standard model which are suppressed by much smaller Yukawa couplings. However the last contribution in (3.68) from sm interactions *may be* of the same order as the bsm contributions for a relevant range of k. To see this note that $\mathbb{A}_R, \mathbb{B}_R \sim Y_2^2 \sim 10^{-16}$, whereas $\mathbb{A}_L, \mathbb{B}_L \sim g^2 \sim 0.4$ therefore with $\bar{M} \sim$ KeV and $k \lesssim 100$ GeV, it is clear that both contributions bsm and sm are of the same order.

The point of maintaining the helicity dependence throughout is that for the case of sterile neutrinos, namely, the propagating modes "2" in the medium, the exchange of standard model vector bosons yields a contribution to the positive helicity and positive energy components, namely, the right-handed component, which could be of the same order of the bsm contributions for small k which is a region of interest for sterile neutrino production.

IV. REAL PARTS: MIXING ANGLES AND MSW RESONANCES

The dispersion relations (real parts of the poles) and the mixing angles in the medium are determined by the real parts of the self-energy, namely, the "index of refraction." Whereas the neutral current tadpole contribution (3.7) is real, the real part of the other contributions is obtained from the dispersive form (3.5), namely,

$$\text{Re}\,\Sigma(k_0, k) = \frac{1}{\pi}\int_{-\infty}^{\infty} d\omega \mathcal{P}\Big(\frac{\text{Im}\Sigma(\omega, \vec{k})}{\omega - k_0}\Big). \qquad (4.1)$$

In general the real part must be obtained numerically and is a function of three parameters k_0, k, μ which makes its exploration a daunting numerical task. However, progress can be made by focusing on the "on shell" contribution, namely, setting $k_0 \simeq k$, and neglecting the dependence on μ, which is warranted in the whole region of k, T of interest, but for k/T, $|\mu|/T \ll M/T$ in which case we provide below an accurate approximate form.

In obtaining the real parts we consider only the finite temperature contribution, because the zero temperature part is absorbed in the renormalization of the parameters in the Lagrangian.

Scalars bsm: For the real part of the scalar bsm self-energy we find for $k_0 = k$; $\mu = 0$

$$\text{Re}\,\Sigma_{\text{bsm}}(k, k) = \frac{Y^2 T}{16\pi^2}\Big\{\gamma^0\Big[Af\Big(\frac{k}{T};\frac{M}{T}\Big) + Ab\Big(\frac{k}{T};\frac{M}{T}\Big)\Big]$$
$$- \vec{\gamma} \cdot \hat{\mathbf{k}}\Big[Bf\Big(\frac{k}{T};\frac{M}{T}\Big) + Bb\Big(\frac{k}{T};\frac{M}{T}\Big)\Big]\Big\}, \qquad (4.2)$$

where Af; Bf and Ab; Bb are the fermionic and bosonic contributions, respectively, and $Y = Y_{1,2}$ for σ, φ exchange. Figures 5 show Af; Bf and Ab; Bb for $M/T = 1, 2, 3$ as a function of k/T.

For $\Sigma_{\sigma,\varphi}^{(2)}$ the intermediate fermion line corresponds to a sterilelike neutrino, therefore for these contributions we must set $Af = 0$; $Bf = 0$, under the assumption that the sterile neutrino population can be neglected and the propagator for the internal line is the vacuum one. For the mixing angle the relevant contribution is $A - B$. Figures 6 display $Af - Bf$ and $Ab - Bb$ for $M/T = 1, 2, 3$ as a function of k/T.

We note that the fermionic and bosonic contributions Af, Ab are qualitatively very similar and the same property holds for Bf, Bb. Therefore neglecting the fermionic contributions both for $\Sigma^{(1)}$ does *not* affect the results and the conclusions in a substantial manner.

This observation confirms that the general results presented below are robust *even* when the neutrinos "1" are not thermalized and their propagators are the vacuum ones.

Although an analytic form for the full range of k_0; k; μ is not available, we obtain an analytic expression for the relevant case k_0/T, k/T, $\mu/T \ll M/T \sim 1$. We find to leading order in the small ratios k_0/T; k/T; $\xi = \mu/T$,
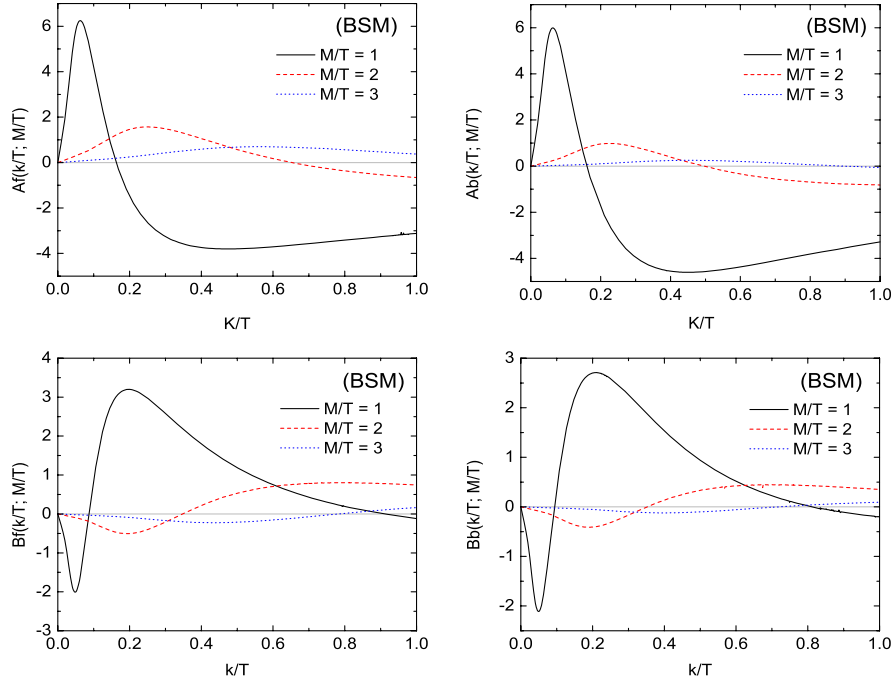
FIG. 5 (color online).   The functions $Af(k/T; M/T)$; $Ab(k/T; M/T)$; $Bf(k/T; M/T)$; $Bb(k/T; M/T)$ as a function of k/T for $M/T = 1, 2, 3$.

$$\mathrm{Re}\Sigma_\sigma^{(1)}(k_0, k) = \frac{Y_1^2 T^2}{M_\sigma^2}\left\{\gamma^0\left[-\frac{T\xi}{12}\left(1+\frac{\xi^2}{\pi^2}\right)\right.\right.$$
$$+\frac{7\pi^2}{120}\frac{k_0 T^2}{M_\sigma^2}[1 + F[M_\sigma/T]]$$
$$\left.\left.-\vec{\gamma}\cdot\hat{k}\left[-\frac{7\pi^2}{360}\frac{kT^2}{M_\sigma^2}[1 + J[M_\sigma/T]]\right]\right\}, \quad (4.3)$$

$$\mathrm{Re}\Sigma_\sigma^{(2)}(k_0, k) = \frac{Y_1^2 T^2}{M_\sigma^2}\left\{\gamma^0\left[\frac{7\pi^2}{120}\frac{k_0 T^2}{M_\sigma^2}F[M_\sigma/T]\right]\right.$$
$$\left.-\vec{\gamma}\cdot\hat{k}\left[-\frac{7\pi^2}{360}\frac{kT^2}{M_\sigma^2}J[M_\sigma/T]\right]\right\}, \quad (4.5)$$

$$\mathrm{Re}\Sigma_\varphi^{(1)}(k_0, k) = \frac{Y_2^2 T^2}{M_\varphi^2}\left\{\gamma^0\left[-\frac{T\xi}{12}\left(1+\frac{\xi^2}{\pi^2}\right)\right.\right.$$
$$+\frac{7\pi^2}{120}\frac{k_0 T^2}{M_\varphi^2}[1 + F[M_\varphi/T]]$$
$$\left.\left.-\vec{\gamma}\cdot\hat{k}\left[-\frac{7\pi^2}{360}\frac{kT^2}{M_\varphi^2}[1 + J[M_\varphi/T]]\right]\right\}, \quad (4.4)$$

$$\mathrm{Re}\Sigma_\varphi^{(2)}(k_0, k) = \frac{Y_2^2 T^2}{M_\varphi^2}\left\{\gamma^0\left[\frac{7\pi^2}{120}\frac{k_0 T^2}{M_\varphi^2}F[M_\varphi/T]\right]\right.$$
$$\left.-\vec{\gamma}\cdot\hat{k}\left[-\frac{7\pi^2}{360}\frac{kT^2}{M_\varphi^2}J[M_\varphi/T]\right]\right\}, \quad (4.6)$$

where

FIG. 6 (color online).   The functions $Af(k/T; M/T) - Bf(k/T; M/T)$; $Ab(k/T; M/T) - Bb(k/T; M/T)$ as a function of k/T for $M/T = 1, 2, 3$.

$$J(m) = \frac{120}{7\pi^4} \int_0^\infty dq \, \frac{q^2}{W_q} N_B(W_q) \left[W_q^2 + \frac{m^2}{2} \right];$$

$$F(m) = \frac{120}{7\pi^4} \int_0^\infty dq \, \frac{q^2}{W_q} N_B(W_q) \left[W_q^2 - \frac{m^2}{2} \right]. \tag{4.7}$$

These functions are displayed in Fig. 9, they are $\mathcal{O}(1)$ in the region of interest $M_{\sigma,\varphi} \sim T$.

A comprehensive numerical study of Af, Ab, Bf, Bb confirms the validity of the above approximations for $k_0 = k$, $\mu = 0$ for $k/T \ll 1$.

Vector bosons sm: Similarly, for the real part of the sm self-energy we find for $k_0 = k$; $\mu = 0$

$$\mathrm{Re}\Sigma_{\mathrm{sm}}(k, k) = \frac{g_{\mathrm{sm}}^2 T}{16\pi^2} \left\{ \gamma^0 \left[Af\left(\frac{k}{T}; \frac{M}{T}\right) + Ab\left(\frac{k}{T}; \frac{M}{T}\right) \right] \right.$$
$$\left. - \vec{\gamma} \cdot \hat{\mathbf{k}} \left[Bf\left(\frac{k}{T}; \frac{M}{T}\right) + Bb\left(\frac{k}{T}; \frac{M}{T}\right) \right] \right\}, \tag{4.8}$$

where we use the same definition, namely, Af; Bf and Ab; Bb are the fermionic and bosonic contributions, respectively. Figures 7 show Af; Bf and Ab; Bb and Fig. 8 shows $Af(k/T; M/T) - Bf(k/T; M/T)$;　　$Ab(k/T; M/T) - Bf(k/T; M/T)$ for $M/T = 1, 2, 3$ as a function of k/T.

Just as in the bsm case analyzed above, we note that the fermionic and bosonic contributions Af; Ab are qualitatively similar and the same holds for Bf; Bb. Again this observation confirms that our results are robust, independently of whether *any* of the neutrino modes are thermalized.
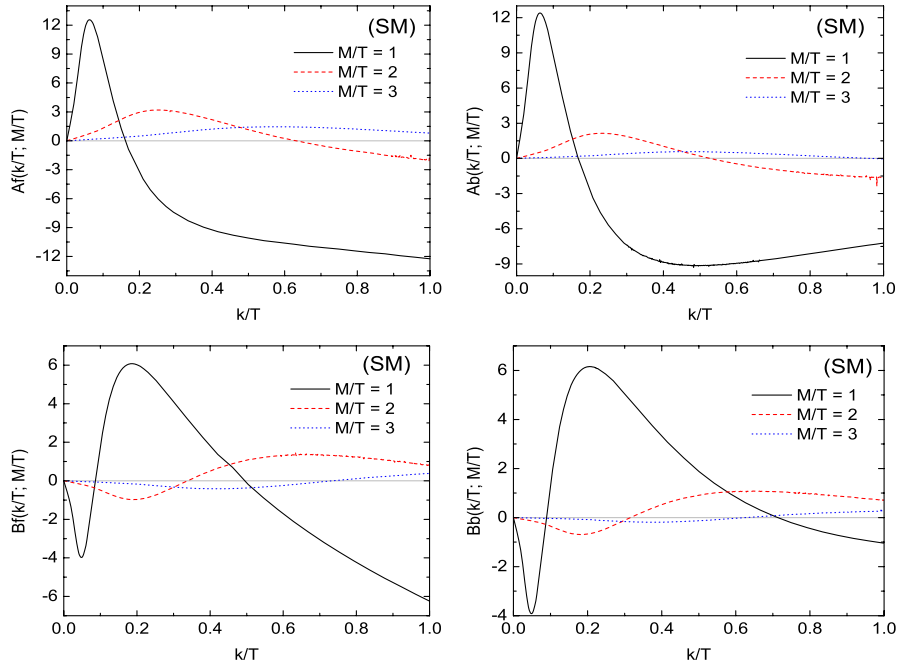
We also obtain the analytic forms for $\mathrm{Re}\Sigma_{\mathrm{sm}}(k_0; k)$ for $k_0/T, k/T, \mu/T \ll M_{W,Z}/T \sim 1$. To leading order in these small ratios we find

$$\mathrm{Re}\Sigma_{nc}^{(1)}(k_0, k) = \frac{g^2 T^2}{4M_W^2} \left\{ \gamma^0 \left[-\frac{T\xi}{4} \left(1 + \frac{\xi^2}{\pi^2} \right) \right. \right.$$
$$\left. + \frac{7\pi^2}{60} \frac{k_0 T^2}{M_Z^2} [1 + G[M_Z/T]] \right]$$
$$\left. - \vec{\gamma} \cdot \hat{k} \left[-\frac{7\pi^2}{180} \frac{kT^2}{M_Z^2} [1 + G[M_Z/T]] \right] \right\}, \tag{4.9}$$

$$\mathrm{Re}\Sigma_{nc}^{(2)}(k_0, k) = \frac{g^2 T^2}{4M_W^2} \left\{ \gamma^0 \left[\frac{7\pi^2}{60} \frac{k_0 T^2}{M_Z^2} G[M_Z/T] \right] \right.$$
$$\left. - \vec{\gamma} \cdot \hat{k} \left[-\frac{7\pi^2}{180} \frac{kT^2}{M_Z^2} G[M_Z/T] \right] \right\}, \tag{4.10}$$

$$\mathrm{Re}\Sigma_{cc,\mathrm{sm}}(k_0, k) = \frac{g^2 T^2}{2M_W^2} \left\{ \gamma^0 \left[\frac{7\pi^2}{60} \frac{k_0 T^2}{M_W^2} [1 + G[M_W/T]] \right] \right.$$
$$\left. - \vec{\gamma} \cdot \hat{k} \left[-\frac{7\pi^2}{180} \frac{kT^2}{M_W^2} [1 + G[M_W/T]] \right] \right\}. \tag{4.11}$$

In the charged current contribution we have neglected the asymmetry of the charged lepton because it is of the order of the baryon asymmetry. In the above expressions

FIG. 7 (color online).　The functions $Af(k/T; M/T)$; $Ab(k/T; M/T)$; $Bf(k/T; M/T)$; $Bb(k/T; M/T)$ as a function of k/T for $M/T = 1, 2, 3$.
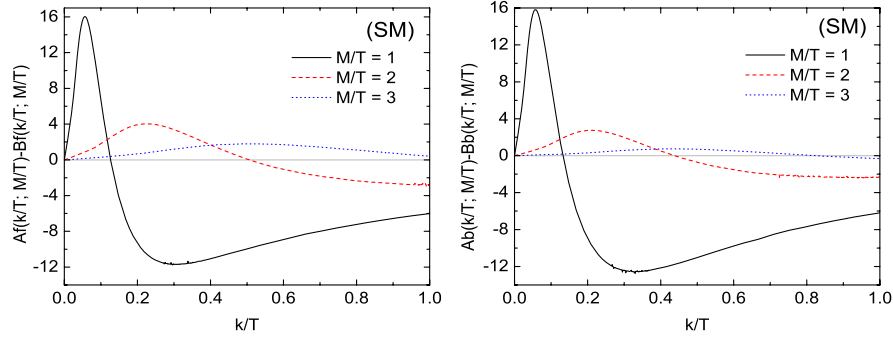
FIG. 8 (color online). The functions $Af(k/T; M/T) - Bf(k/T; M/T)$; $Ab(k/T; M/T) - Bb(k/T; M/T)$ as a function of k/T for $M/T = 1, 2, 3$.

$$G[m] = \frac{120}{7\pi^4} \int_0^\infty dq \frac{q^2}{W_q} N_B(W_q)\left[W_q^2 - \frac{m^2}{4}\right];$$

$$N_B(W_q) = \frac{1}{e^{W_q} - 1}; \qquad W_q = \sqrt{q^2 + m^2}. \tag{4.12}$$

This function is depicted in Fig. 9, it is $\mathcal{O}(1)$ in the region of interest $T \sim M_{Z,W}$.

The validity of these approximations for $k_0 = k$, $\mu = 0$ is confirmed by the numerical analysis of Af, Ab, Bf, Bb for $k/T \ll 1$.

It is remarkable that the leading order in k_0/T, k/T but for $M_{W,Z} \sim T$ reproduce the results of Refs. [53,54] which were obtained in the low energy limit T, $\mu \ll M_{W,Z}$. The numerical analysis carried out for $k_0 = k$; $\mu = 0$ confirms that for $M/T \gg 1$ the range of validity of the lowest order approximation in k/T increases and merges with the results given above in Eqs. (4.3), (4.4), (4.5), (4.6), (4.7), (4.8), (4.9), (4.10), and (4.11) up to $k/T \sim 1$.
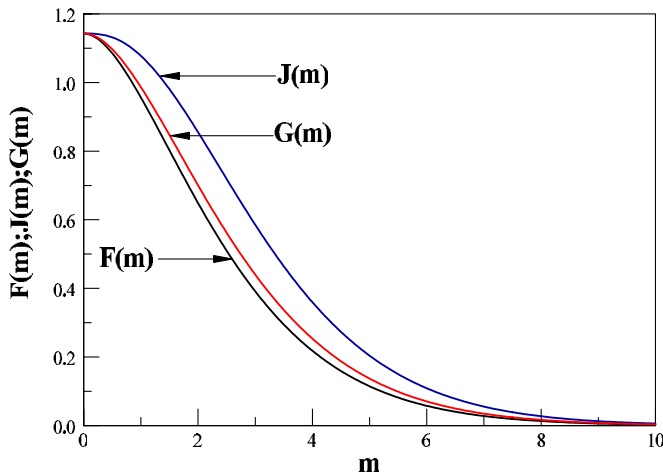
FIG. 9 (color online). The functions $F(m)$; $J(m)$; $G(m)$ vs. $m = M/T$.

A. Mixing angles and MSW resonances:

As shown in detail in the previous sections, the mixing angle in the medium θ_m determined by the relations (3.47) depends on k_0, k, and the helicity h. On the mass shell of the propagating modes in the medium we can replace $k_0 \simeq k$ in the expressions for the real part of the matrices $\text{Re}\mathbb{A}$; $\text{Re}\mathbb{B}$ for Δ_R, namely, the real part of Eqs. (3.66) and (3.68), for $h = \mp 1$, respectively. For $\mu = 0$; $k_0 = k$ and general k, M the fermionic and bosonic contributions to the real parts of the bsm self-energies are given by Eq. (4.2) where the fermionic (Af, Bf) and bosonic (Ab, Bb) contributions are depicted in Figs. 5 and 6. The real parts of the sm self-energies are given by Eq. (4.8) and the fermionic and bosonic contributions depicted in Figs. 7 and 8.

These figures distinctly show that the contributions Af, Ab and Bf, Bb for bsm and sm self-energies are qualitatively the same, with only a quantitative difference in the amplitudes. A remarkable result is that these functions *change sign*. In particular the combinations $Af - Bf$, $Ab - Bb$ which enter in Δ_R change sign at a value of k/T that depends on the ratio M/T. For $M/T \sim 1$ these differences vanish at $k/T \simeq 0.2$. A numerical exploration reveals that the sign change persists until $M/T \simeq 3$ but occurs at monotonically larger values of k/T. This behavior is shown in the figures above. We find that for $M/T \gtrsim 3$ the change in sign occurs for $k \gg T$ or does not occur at all. On the mass shell $k_0 \sim k$ and for $\mu = 0$ this study reveals that Δ_R is *negative* in a wide region of momentum for $M/T \lesssim 1$. This fact entails that there are MSW resonances near the momentum regions where the coefficient functions change sign, even in the *absence of a lepton asymmetry*. To understand this important point more clearly let us study the case $h = \mp 1$ separately.

$h = -1$: In this case Δ is given by Eq. (3.66), furthermore from Eq. (3.13) it follows that $(\mathbb{A}_L - \mathbb{B}_L)_{ss}$ is determined by the bsm contributions which are suppressed by small Yukawa couplings $Y \lesssim 10^{-8}$ as compared to the sm contributions. Therefore the bsm contribution can be neglected and Δ_R is determined by the sm contributions given by Eqs. (4.8), furthermore approximating $\cos(\theta) \sim 1$;

$\sin(\theta) \sim 0$ in Eq. (3.12) and $\delta M^2 \simeq M_s^2$, we find (for $\mu = 0$; $h = -1$)

$$\Delta_R(k) \simeq \frac{g^2}{16\pi^2}\left(\frac{T}{M_s}\right)^2\left(\frac{k}{T}\right)\left\{\left[Af\left(\frac{k}{T}, \frac{M_W}{T}\right) + Ab\left(\frac{k}{T}, \frac{M_W}{T}\right)\right.\right.$$
$$\left. - Bf\left(\frac{k}{T}, \frac{M_W}{T}\right) - Bb\left(\frac{k}{T}, \frac{M_W}{T}\right)\right]$$
$$+ \frac{1}{2\cos(\theta_w)}\left[Af\left(\frac{k}{T}, \frac{M_Z}{T}\right) + Ab\left(\frac{k}{T}, \frac{M_Z}{T}\right)\right.$$
$$\left.\left. - Bf\left(\frac{k}{T}, \frac{M_Z}{T}\right) - Bb\left(\frac{k}{T}, \frac{M_Z}{T}\right)\right]\right\}. \quad (4.13)$$

Taking as representative $T \sim 100$ GeV; $M_s \sim$ keV it follows that

$$\frac{g^2}{16\pi^2}\left(\frac{T}{M_s}\right)^2 \simeq 2.7 \times 10^{13}. \quad (4.14)$$

Figures. 8 show that for $M_{W,Z}/T \lesssim 3$ there is a region in k/T in which the bracket in (4.13) is *negative* and there is a value $(k/T)_c$ that increases with M/T at which the bracket vanishes, for example, from the Fig. 8 we find $(k/T)_c \sim 0.2$; 0.45; 1 for $M/T \sim 1, 2, 3$, respectively. For $k/T < (k/T)_c$ the bracket is positive (for $\mu = 0$) whereas for $k/T > (k/T)_c$ it is *negative*, therefore there is a value of k/T at which the resonance condition (3.49) is fulfilled. Since the coefficient of the bracket is $\approx 10^{13}$ [Eq. (4.14)] and the terms inside the bracket are of $\mathcal{O}(1)$ for $k/T \lesssim 1$, and $\cos(\theta) \sim 1$ it follows that the MSW resonance occurs for a value of k/T such that the bracket $\sim 10^{-13}$, namely, for $k/T \sim (k/T)_c$. The large coefficient (4.14) results in a *very narrow* MSW resonance as can be seen as follows, expanding Δ_R near $(k/T)_c$ as

$$\Delta_R(k) \simeq -\kappa\left(\left(\frac{k}{T}\right) - \left(\frac{k}{T}\right)_c\right) + \cdots; \qquad \kappa > 0, \quad (4.15)$$

where $\kappa \gtrsim 10^{13}$ for $M_{W,Z}/T \lesssim 3$ (see Fig. 8) and approximating $\cos(2\theta) \sim 1$ we find

$$\sin^2(2\theta_m) \simeq \frac{\epsilon^2}{\left[\left(\left(\frac{k}{T}\right) - \left(\frac{k}{T}\right)_c - \frac{1}{\kappa}\right)^2 + \epsilon^2\right]};$$
$$\epsilon = \sin(2\theta)/\kappa. \quad (4.16)$$

For example taking $\sin(2\theta) \sim 10^{-5}$ [48] it follows that $\epsilon \lesssim 10^{-18}$ which makes the resonance very narrow. During cosmological expansion the ratio $M/T(t)$ increases with the scale factor, while the ratio k/T (with k the physical momentum) is fixed. Therefore, for a fixed value of $k/T < 1$ as M/T increases the resonance is crossed very sharply.

$h = 1$: To assess the possibility of MSW resonances for $h = 1$ we need the real part of (3.68). From (3.12) and (4.2) it follows that $(\mathbb{A}_R - \mathbb{B}_R)_{aa} \propto Y_1^2$; $(\mathbb{A}_R - \mathbb{B}_R)_{ss} \propto Y_2^2$, since $Y_2 \gg Y_1$ we can neglect the first term (corresponding to σ exchange). Similarly in the term $(\mathbb{A}_R - \mathbb{B}_R)_{ss}$ we neglect the contribution from σ exchange and approximate $\cos(\theta) \sim 1$; $\sin(\theta) \sim 0$ in (3.13), hence only $\Sigma_\varphi^{(2)}$ contrib-

utes to Σ_{ss}. Furthermore, approximating $\delta M^2 \sim \bar{M}^2 \sim M_s^2$ we finally find for $h = 1$; $\mu = 0$,

$$\Delta_R(k) \simeq -\left(\frac{Y_2 T}{\sqrt{8}\pi M_s}\right)^2\left(\frac{k}{T}\right)\left[Ab\left(\frac{k}{T}, \frac{M_\varphi}{T}\right) - Bb\left(\frac{k}{T}, \frac{M_\varphi}{T}\right)\right]$$
$$+ \frac{g^2}{128\pi^2}\left(\frac{T}{k}\right)\left\{\left[Af\left(\frac{k}{T}, \frac{M_W}{T}\right) + Ab\left(\frac{k}{T}, \frac{M_W}{T}\right)\right.\right.$$
$$\left. + Bf\left(\frac{k}{T}, \frac{M_W}{T}\right) + Bb\left(\frac{k}{T}, \frac{M_W}{T}\right)\right] + \frac{1}{2\cos(\theta_w)}$$
$$\times \left[Af\left(\frac{k}{T}, \frac{M_Z}{T}\right) + Ab\left(\frac{k}{T}, \frac{M_Z}{T}\right) + Bf\left(\frac{k}{T}, \frac{M_Z}{T}\right)\right.$$
$$\left.\left. + Bb\left(\frac{k}{T}, \frac{M_Z}{T}\right)\right]\right\}, \quad (4.17)$$

where in the first line the Ab; Bb are bsm displayed in Figs. 5.

We note that with $T \sim 100$ GeV, $M_s \sim$ KeV the value of the Y_2 [see Eq. (2.10)] is such that $Y_2 T/M_s \sim \mathcal{O}(1)$, therefore Fig. 6 (right panel) suggests that the bsm contribution may yield an MSW resonance in the region $k/T \lesssim 0.15$; $M_\varphi \sim T$, where the bsm contribution $Ab - Bb$ is *positive* and large. Since $g^2/128\pi^2 \sim 3.4 \times 10^{-4}$ and $Af + Bf$; $Ab + Bb \sim \mathcal{O}(1)$ for $k/T \lesssim 1$ it follows that the sm contribution to Δ_R is *subleading* for $k/T \lesssim 1$ and the bsm contribution *may* lead to an MSW resonance in this region depending on the parameters of the extension bsm.

$\mu \neq 0$; $k/T \ll M/T \sim 1$:

The above results are valid for $\mu = 0$, for $\mu \neq 0$ a full numerical evaluation of the real parts of the kernel is not available, however, the bounds on the lepton asymmetry from Ref. [60] suggest that $|\mu/T| \lesssim 0.02 \ll 1$ and we can obtain a reliable understanding of the influence of the lepton asymmetry (in the neutrino sector) by focusing on the region of $k/T \ll 1$, in which we can use the results (4.3), (4.4), (4.5), and (4.6) for bsm and (3.7) along with (4.9), (4.10), and (4.11) for sm and approximate $\cos(\theta) \sim 1$; $\sin(\theta) \sim 0$ in (3.12) and (3.13), and $\delta M^2 \sim M_s^2$.

For $h = -1$ again we neglect the bsm contributions to $\Delta_R(k)$ in (3.66), and for μ/T; $k/T \ll 1$ we obtain,

$$\Delta_R(k) \simeq \frac{g^2 T^3 k}{M_W^2 M_s^2}\left\{-\frac{5\xi}{24} + \frac{7\pi^2}{90}\left(\frac{k}{T}\right)\left[\left(\frac{T}{M_Z}\right)^2\left(1 + G\left(\frac{M_Z}{T}\right)\right)\right.\right.$$
$$\left.\left. + 2\left(\frac{T}{M_W}\right)^2\left(1 + G\left(\frac{M_W}{T}\right)\right)\right]\right\}. \quad (4.18)$$

We note that for $T \sim M_W$; $M_s \sim$ KeV the prefactor

$$\frac{g^2 T^3 k}{M_W^2 M_s^2} \sim 10^{16}\left(\frac{k}{T}\right) \quad (4.19)$$

and the resonance condition (3.49) can be fulfilled for $\xi > 0$ when the bracket in (4.18) approximately vanishes, namely, for

$$\left(\frac{k}{T}\right) \sim \frac{25\xi}{56\pi^2} \Rightarrow k \sim 0.05\mu, \quad (4.20)$$

where we have used $G(M_{W,Z}/T) \sim 1$ for $T \sim M_W$, a result that can be gleaned from Fig. 9. For $\xi > 0$ this MSW resonance occurs for antineutrinos (namely, $k_0 = -k$), a result that follows from the relations (3.61) and (3.62).

Similarly, for $h = 1$ and μ/T, $k/T \ll 1$, we obtain

$$\Delta_R(k) \simeq -\left(\frac{Y_2^2 T^2}{M_s^2}\right)\left(\frac{T^4}{M_\varphi^4}\right)\left(\frac{k^2}{T^2}\right)\frac{7\pi^2}{180}\left[J\left(\frac{M_\varphi}{T}\right) + 3F\left(\frac{M_\varphi}{T}\right)\right]$$
$$+ \frac{g^2 T^2}{M_W^2}\left(\frac{T}{k}\right)\left\{-\frac{5\xi}{192} + \frac{7\pi^2}{1440}\left(\frac{k}{T}\right)\left[\left(\frac{T}{M_Z}\right)^2\left(1 + G\right.\right.\right.$$
$$\left.\left.\left.\times\left(\frac{M_Z}{T}\right)\right) + 2\left(\frac{T}{M_W}\right)^2\left(1 + G\left(\frac{M_W}{T}\right)\right)\right]\right\}. \quad (4.21)$$

Obviously, there is a competition between sm and bsm contributions in Eq. (4.21). When $T \sim M_{W,Z,\varphi}$, $J(1)$, $F(1)$, $G(1) \sim 1$, and $(Y_2^2 T^2)/M_s^2 \sim 1$. Therefore, the bsm contribution to $\Delta_R(k)$ is

$$\Delta_R^{\text{(bsm)}} \sim -\frac{7\pi^2}{45}\left(\frac{k}{T}\right)^2 = -1.54\left(\frac{k}{T}\right)^2, \quad (4.22)$$

and the sm contribution to $\Delta_R(k)$ reads

$$\Delta_R^{\text{(sm)}} \sim 0.1\left(\frac{T}{k}\right)\left[-\frac{5\xi}{192} + \left(\frac{k}{T}\right)\frac{7\pi^2}{240}\right]$$
$$\sim 0.029 - 3 \times 10^{-3}\left(\frac{T}{k}\right)\xi. \quad (4.23)$$

The resonance happens for $\Delta_R(k) \sim -1$, namely,

$$3 \times 10^{-3}\left(\frac{T}{k}\right)\xi \sim 1.029. \quad (4.24)$$

Obviously, one is always able to find a value of k/T to satisfy Eq. (4.24) for any given positive lepton asymmetry ξ. For $|\xi| \sim 10^{-2}$ consistent with the WMAP and BBN data [60], we obtain

$$\frac{k}{T} \sim 3 \times 10^{-3}\xi \sim 3 \times 10^{-5}. \quad (4.25)$$

Note that the asymmetry term from sm contribution dominates over the bsm contribution, which is different from $\mu = 0$ case where bsm contribution would dominate as shown in (4.17). This analysis leads us to conclude that for a lepton asymmetry hidden in the neutrino sector compatible with the bounds from Ref. [60] there is the possibility of *two* MSW resonances.

V. IMAGINARY PARTS: WIDTHS FROM VECTOR AND SCALAR BOSON DECAY

The quasiparticle widths $\Gamma_{1,2}(k)$ are given by Eqs. (3.57) and (3.60). Analyzing the explicit expressions for the imaginary parts of the sm and bsm contributions given in the appendix, Eqs. (A1)–(A3) and (B1)–(B3), respectively, the "on shell" contributions are obtained from those whose δ function constraints can be satisfied for $\omega \sim k$. It is straightforward to find that *only* the terms with $\delta(\omega + p -$

$W_{\vec{p}+\vec{k}})$ have nonvanishing support for $\omega \simeq k$. These terms are given in the last lines of (A2) and (A3) for sm and the last lines of (B2) and (B3) for bsm contributions.

These contributions to the quasiparticle widths in the medium arise from the *decay* of the intermediate boson, either the vector bosons in the sm contributions or the scalars in the bsm contributions. This is depicted in Fig. 10, the Cutkosky cut through the intermediate boson (vector or scalar) yields the imaginary part. The process that contributes on shell $\omega \simeq k$ is the decay of the boson into the fermions (neutrinos and or charged leptons) depicted in this figure.

The fact that the decay of a heavy intermediate state leads to a width was recognized in Ref. [58].

The analysis of the different cases is simplified by introducing

$$\Gamma_{aa}(k_0, k) = \text{Im}\left[\frac{(k_0 + hk)}{2k}(\mathbb{A}_R - h\mathbb{B}_R)_{aa}\right.$$
$$\left. + \frac{(k_0 - hk)}{2k}(\mathbb{A}_L + h\mathbb{B}_L)_{aa}\right], \quad (5.1)$$

$$\Gamma_{ss}(k_0, k) = \text{Im}\left[\frac{(k_0 + hk)}{2k}(\mathbb{A}_R - h\mathbb{B}_R)_{ss}\right.$$
$$\left. + \frac{(k_0 - hk)}{2k}(\mathbb{A}_L + h\mathbb{B}_L)_{ss}\right], \quad (5.2)$$

in terms of which [see Eq. (3.32)]

$$S_I = 2k[\Gamma_{aa}(k_0, k) + \Gamma_{ss}(k_0, k)];$$
$$\Delta_I(k_0, k) = \frac{2k}{\delta M^2}[\Gamma_{aa}(k_0, k) - \Gamma_{ss}(k_0, k)]. \quad (5.3)$$

We need these quantities evaluated on the "mass shell", namely, for positive energy $k_0 = \bar{\omega}(k) \sim k + \bar{M}^2/2k$. We find:

$h = -1$:

$$\Gamma_{aa}(k) \simeq \text{Im}(\mathbb{A}_L - \mathbb{B}_L)_{aa}; \qquad \Gamma_{ss}(k) \simeq \text{Im}(\mathbb{A}_L - \mathbb{B}_L)_{ss}. \quad (5.4)$$

$h = 1$:

$$\Gamma_{aa}(k) \simeq \text{Im}\left[(\mathbb{A}_R - \mathbb{B}_R)_{aa} + \frac{\bar{M}^2}{4k^2}(\mathbb{A}_L + \mathbb{B}_L)_{aa}\right];$$
$$\Gamma_{ss}(k) \simeq \text{Im}(\mathbb{A}_R - \mathbb{B}_R)_{ss}. \quad (5.5)$$

In the above expressions we have used $Y_{1,2} \ll g$ and $\bar{M}^2/4k^2 \ll 1$ and neglected terms accordingly, we have suppressed the arguments on $\mathbb{A}$, $\mathbb{B}$, however, these matrix elements depend on k. The term with $\mathbb{A}_L + \mathbb{B}_L$ in (5.5) is noteworthy: the leading contribution to this term is from sm interactions, even setting the Yukawa couplings in the bsm sector to zero a *nearly right-handed sterile neutrino is produced via the decay of the vector bosons.*

The expression for the imaginary parts (3.57) and (3.60) simplify in two relevant limits [63]:

(a) *weak damping*: $|\tilde{\gamma}| \ll 1$: in this limit we find

$$r\sin(\phi) \simeq \tilde{\gamma}\cos2\theta_m \qquad (5.6)$$

leading to the following results for the poles with positive energy:

$$\Gamma_1(k) = \Gamma_{aa}(k)\cos^2\theta_m + \sin^2\theta_m\Gamma_{ss}(k), \qquad (5.7)$$

$$\Gamma_2(k) = \Gamma_{aa}(k)\sin^2\theta_m + \cos^2\theta_m\Gamma_{ss}(k). \qquad (5.8)$$

Furthermore the difference in the dispersion relations becomes

$$\Delta\Omega_{\mathrm{wd}} \equiv \Omega_2(k) - \Omega_1(k) \simeq \frac{\delta M^2}{2k}\rho_0, \qquad (5.9)$$

which is the usual result for neutrino mixing.

(b) *Strong damping*: $|\tilde{\gamma}| \gg 1$, in this limit we find

$$r\sin(\phi) \simeq \tilde{\gamma}\,\mathrm{sign}(\cos(2\theta_m))\left[1 - \frac{\sin^2(2\theta_m)}{2\tilde{\gamma}^2}\right] \qquad (5.10)$$

leading to the following results:

$$\Gamma_1(k) = \frac{1}{2}(\Gamma_{aa}(k) + \Gamma_{ss}(k)) + \frac{1}{2}(\Gamma_{aa}(k) - \Gamma_{ss}(k))$$
$$\times\left(\mathrm{sign}(\cos(2\theta_m)) - \frac{\sin^2(2\theta_m)}{2\tilde{\gamma}^2}\right), \qquad (5.11)$$

$$\Gamma_2(k) = \frac{1}{2}(\Gamma_{aa}(k) + \Gamma_{ss}(k)) - \frac{1}{2}(\Gamma_{aa}(k) - \Gamma_{ss}(k))$$
$$\times\left(\mathrm{sign}(\cos(2\theta_m)) - \frac{\sin^2(2\theta_m)}{2\tilde{\gamma}^2}\right). \qquad (5.12)$$

In this case the frequency difference between the propagating states becomes

$$\Delta\Omega_{\mathrm{sd}} \equiv \Omega_2(k) - \Omega_1(k) \simeq \frac{\delta M^2}{2k}\rho_0|\cos(2\theta_m)|$$
$$= \frac{\delta M^2}{2k}|\cos(2\theta) + \Delta_R(k)|. \qquad (5.13)$$

This is a remarkable result, the frequency difference *vanishes* at an MSW resonance in striking contrast with the usual quantum mechanics description of neutrino mixing and oscillations wherein there is a "level repulsion" at an MSW resonance that prevents level crossing.

In all the expressions above $\Gamma_{aa}(k); \Gamma_{ss}(k)$ are given by (5.4) and (5.5) in the respective cases $h = \mp 1$, and the mixing angle θ_m is obtained from Eqs. (3.47) evaluating Δ_R at $k_0 = k$.

The widths for negative energy and $h = \mp 1$ are obtained from the expressions above by the replacement $\mu \to -\mu$, this is a consequence of the relations (3.61) and (3.62) and the fact that the chemical potential is *CP*-odd, therefore the particle and antiparticle widths only differ because of the chemical potential.

We emphasize that the results (5.7), (5.8), (5.11), and (5.12) are *general*, and hold to *all orders* in perturbation theory as they follow from the general form of the self-energies. In particular these relations are valid beyond the one-loop order studied here and hold for *any* processes that contributes to the absorptive parts of the self-energy at one-loop or higher order.

A. Widths from scalar and vector boson decay:

As discussed above, the imaginary parts of the self-energy are given in the Appendix, both for sm and bsm contributions. Inspection of the different delta functions shows that the *only* contribution "on shell", namely, $\omega \simeq k$ arises from the terms with $\delta(\omega + p - W_{\vec{p}+\vec{k}})$ in the expressions for the imaginary parts (B2) and (B3).

This delta function corresponds to a Cutkosky cut that describes the process of a scalar (in bsm) or a vector (in sm) boson *decay* into a neutrino and another lepton, displayed in Fig. 10.

Scalars bsm: For scalars the (R) and (L) components are the same. We find for $Y = Y_{1,2}$; $M = M_{\sigma,\varphi}$ for σ, φ exchange, respectively,

$$\mathrm{Im}\,(\mathbb{A}_R - \mathbb{B}_R) = \mathrm{Im}(\mathbb{A}_L - \mathbb{B}_L)$$
$$= \frac{Y^2 T}{32\pi}\frac{M^2}{k^2}\ln\left[\frac{1 + C_1 e^{-x^*-\xi}}{1 - e^{-x^*-y}}\right], \qquad (5.14)$$

where

$$x^* = \frac{M^2}{4kT}; \qquad \xi = \frac{\mu}{T}; \qquad y = \frac{k}{T}, \qquad (5.15)$$

and

$$C_1 = \begin{cases} 1 & \text{for } \Sigma_{\sigma,\varphi}^{(1)}, \\ 0 & \text{for } \Sigma_{\sigma,\varphi}^{(2)}. \end{cases} \qquad (5.16)$$

In the relevant region $k < M_{\sigma,\varphi} \sim T$ we can safely neglect the contribution from the leptonic chemical potential in (5.14) and set $\xi = 0$, since the bounds from Ref. [60] suggest that $|\xi| \lesssim 0.02$. The result (5.14) agrees with that
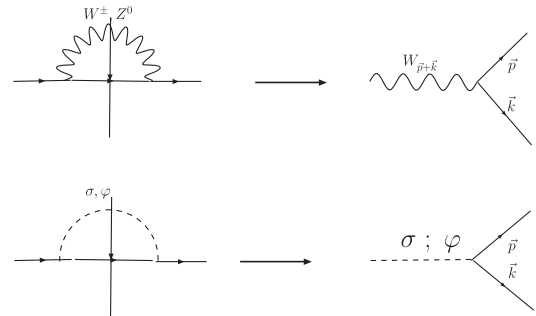
FIG. 10. The Cutkosky cut for imaginary part of the sm and bsm contributions, and the contribution on the mass shell $\omega \simeq k$.

found in Ref. [43] for the decay of the scalar boson into sterile neutrinos (2) ($C_1 = 0$) for vanishing chemical potential.

For $k/T \ll M/T \sim 1$ we can approximate

$$\text{Im}\,(\mathbb{A}_R - \mathbb{B}_R) = \text{Im}(\mathbb{A}_L - \mathbb{B}_L)$$

$$= \frac{Y^2 T}{32\pi} \frac{M^2}{k^2} e^{-x^*}(C_1 + e^{-y}). \quad (5.17)$$

Vector bosons sm: For sm vector boson exchange (only L), the imaginary parts "on shell" are obtained from the terms with $\delta(\omega + p - W_{\vec{p}+\vec{k}})$ in the imaginary parts (A2) and (A3) setting $\omega \simeq k$. We find

$$\text{Im}\,(\mathbb{A}_L - \mathbb{B}_L) = \frac{g_{sm}^2 T}{16\pi} \frac{M^2}{k^2} \ln\left[\frac{1 + C_2 e^{-x^*-\xi}}{1 - e^{-x^*-y}}\right], \quad (5.18)$$

where g_{sm} is given by Eq. (3.16), $M = M_{Z,W}$ for neutral and charged current contributions, respectively, and

$$C_2 = \begin{cases} 1 & \text{for } \Sigma_{nc}^{(1)}, \Sigma_{cc} \\ 0 & \text{for } \Sigma_{nc}^{(2)} \end{cases}. \quad (5.19)$$

For positive energy, and positive helicity (right-handed), we also need [see Eq. (5.5)]

$$\text{Im}\,(\mathbb{A}_L + \mathbb{B}_L) = \frac{g_{sm}^2 T}{8\pi}\left\{\ln\left[\frac{1 + C_2 e^{-x^*}}{1 - e^{-x^*-y}}\right] + \frac{2T}{k}\right.$$
$$\left. \times \left[\text{Li}_2(e^{-x^*-y}) - C_2 \text{Li}_2(-e^{-x^*})\right]\right\}, \quad (5.20)$$

where Li_2 is the dilogarithm or Spence's function and we have set $\mu = 0$. This expression simplifies in the limit $k/T \ll M/T \sim 1$ with the result

$$\text{Im}\,(\mathbb{A}_L + \mathbb{B}_L) \simeq \frac{g_{sm}^2 T^2}{4\pi k} e^{-x^*}(C_2 + e^{-y}). \quad (5.21)$$

In the above results for vector bosons $M = M_{W,Z}$, respectively.

We can now gather all the results needed for $\Gamma_{aa}(k)$; $\Gamma_{ss}(k)$ (5.4) and (5.5) and the quasiparticle widths $\Gamma_{1,2}(k)$ obtained from them. Approximating $\cos(\theta) \sim 1$; $\sin(\theta) \sim 0$ we find,

$$\text{Im}\,(\mathbb{A}_R - \mathbb{B}_R)_{aa} = \frac{Y_1^2 T}{32\pi}\left(\frac{M_\sigma^2}{k^2}\right)\ln\left[\frac{1}{1 - e^{-x_\sigma^* e^{-y}}}\right]; \quad (5.22)$$

$$\text{Im}(\mathbb{A}_R - \mathbb{B}_R)_{ss} = \text{Im}(\mathbb{A}_L - \mathbb{B}_L)_{ss}$$
$$= \frac{Y_1^2 T}{32\pi}\left(\frac{M_\sigma^2}{k^2}\right)\ln\left[\frac{1 + e^{-x_\sigma^*}}{1 - e^{-x_\sigma^* e^{-y}}}\right]$$
$$+ \frac{Y_2^2 T}{32\pi}\left(\frac{M_\varphi^2}{k^2}\right)\ln\left[\frac{1}{1 - e^{-x_\varphi^* e^{-y}}}\right]; \quad (5.23)$$

$$\text{Im}(\mathbb{A}_L - \mathbb{B}_L)_{aa} = \frac{g^2 T}{32\pi}\left\{\frac{1}{2\cos^2(\theta_w)}\left(\frac{M_Z^2}{k^2}\right)\right.$$
$$\times \ln\left[\frac{1 + e^{-x_Z^*}}{1 - e^{-x_Z^* e^{-y}}}\right]$$
$$+ \left(\frac{M_W^2}{k^2}\right)\ln\left[\frac{1 + e^{-x_W^*}}{1 - e^{-x_W^* e^{-y}}}\right]\right\}$$
$$+ \frac{Y_1^2 T}{32\pi}\left(\frac{M_\sigma^2}{k^2}\right)\ln\left[\frac{1}{1 - e^{-x_\sigma^* e^{-y}}}\right]; \quad (5.24)$$

$$\text{Im}(\mathbb{A}_L + \mathbb{B}_L)_{aa} = \frac{g^2 T}{16\pi}\left\{\frac{1}{2\cos^2(\theta_w)}\left[\ln\left(\frac{1 + e^{-x_Z^*}}{1 - e^{-x_Z^* e^{-y}}}\right)\right.\right.$$
$$\left. + \frac{2T}{k}\left[\text{Li}_2(e^{-x_Z^* e^{-y}}) - \text{Li}_2(-e^{-x_Z^*})\right]\right]$$
$$+ \ln\left(\frac{1 + e^{-x_W^*}}{1 - e^{-x_W^* e^{-y}}}\right) + \frac{2T}{k}\left[\text{Li}_2(e^{-x_W^* e^{-y}})\right.$$
$$\left.\left. - \text{Li}_2(-e^{-x_W^*})\right]\right\} + \frac{Y_1^2 T}{16\pi}\left(\frac{2T}{k}\right)\text{Li}_2(e^{-x_\sigma^* e^{-y}}).$$
$$(5.25)$$

In the expressions above we have defined

$$x_\alpha^* = \frac{M_\alpha^2}{4kT}; \qquad \alpha = \sigma, \varphi, Z, W. \quad (5.26)$$

For small values of the arguments $\text{Li}_2(z) \sim z$ which may be used appropriately whenever $x_\alpha^* > 1$, a situation which describes the relevant range $M_\alpha \sim T$; $k < T$.

Equations. (5.22), (5.23), (5.24), and (5.25) combined with (5.4) and (5.5) yield the complete expressions for the quasiparticle widths $\Gamma_{1,2}$ in all cases, and as per the discussion below, the production rates.

B. Imaginary parts: from the width to the production rates

The connection between the quasiparticle widths (imaginary part of the self-energy "on shell") and the production rate is established via the Boltzmann equation for the production of a given species, in this case that of a "sterile" neutrino. Consider as an example the scalar vertex $Y_1 \bar{\nu}_s \sigma \nu_a$, the analysis is similar for the other, including sm vertices. The Boltzmann equation is of the form (gain) − (loss) (see, for example, the appendix in Ref. [43]). The gain term corresponds to the *decay* process $\sigma \rightarrow \bar{\nu}_a + \nu_s$ and is of the form [43]

$$\frac{dn_s(k)}{dt}\bigg|_{\text{gain}} = \int \frac{d^3 p}{(2\pi)^3} |\mathcal{M}_{fi}|^2 \delta(W_{\vec{p}+\vec{k}} - p - k)$$
$$\times N_B(W_{\vec{p}+\vec{k}})(1 - \bar{n}_F(p))(1 - n_s(k)), \quad (5.27)$$

where N_B, n_F are the bosonic and fermionic distribution functions, respectively. The loss term describes the inverse

process, namely, the recombination $\bar{\nu}_a + \nu_s \rightarrow \varphi$ with

$$
\frac{dn_s(k)}{dt}\bigg|_{\text{loss}} = \int \frac{d^3p}{(2\pi)^3} |\mathcal{M}_{fi}|^2 \delta(W_{\vec{p}+\vec{k}} - p - k)
$$
$$
\times [1 + N_B(W_{\vec{p}+\vec{k}})]\bar{n}_F(p)n_s(k). \qquad (5.28)
$$

Therefore the Boltzmann equation is of the form

$$
\frac{dn_s(k)}{dt} = \int \frac{d^3p}{(2\pi)^3} |\mathcal{M}_{fi}|^2 \delta(W_{\vec{p}+\vec{k}} - p - k)
$$
$$
\times \{N_B(W_{\vec{p}+\vec{k}})(1 - \bar{n}_F(p))(1 - n_s(k))
$$
$$
- [1 + N_B(W_{\vec{p}+\vec{k}})]\bar{n}_F(p)n_s(k)\}. \qquad (5.29)
$$

If the distribution function of the particle in question is slightly perturbed *off equilibrium*, the relaxation rate of the distribution function towards equilibrium is obtained by writing $n_s(k) = n_s^{\text{eq}}(k) + \delta n_s(k)$ and linearizing the Boltzmann equation in $\delta n_s(k)$ [59]. The linearized Boltzmann equation reads

$$
\frac{d\delta n_s(k)}{dt} = -\Gamma_{\text{rel}}\delta n_s(k), \qquad (5.30)
$$

where

$$
\Gamma_{\text{rel}} = \int \frac{d^3p}{(2\pi)^3} |\mathcal{M}_{fi}|^2 \delta(W_{\vec{p}+\vec{k}} - p - k)
$$
$$
\times [\bar{n}_F(p) + N_B(W_{\vec{p}+\vec{k}})]. \qquad (5.31)
$$

As discussed in Ref. [59], the relaxation rate Γ_{rel} is *twice* the quasiparticle width [59] since the distribution function is bilinear in the fields. The relation between Γ_{rel} and the on-shell width becomes evident comparing the expression (5.31) with the "on-shell" imaginary parts, namely, the last lines in Eqs. (A2), (A3), (B2), and (B3) with $\omega \simeq k$. The production rate of the sterile species is obtained by neglecting the inverse process and neglecting the sterile population buildup in the Boltzmann Eq. (5.29), namely,

$$
\frac{dn_s(k)}{dt}\bigg|_{\text{prod}} = \int \frac{d^3p}{(2\pi)^3} |\mathcal{M}_{fi}|^2 \delta(W_{\vec{p}+\vec{k}} - p - k)
$$
$$
\times N_B(W_{\vec{p}+\vec{k}})(1 - \bar{n}_F(p)). \qquad (5.32)
$$

Therefore by obtaining the bosonic and fermionic contributions to the quasiparticle widths as in the previous section, we can obtain the production rate. Although the term with the product $N_B\bar{n}_F$ is not included in the width, such term is smaller than the term with N_B only, since $p^2\bar{n}_F(p)$ features a maximum at $p/T \sim 2.3$ for which $\bar{n}_F(p) \sim 0.09$ (for $\mu/T \ll 1$). Therefore in the region of importance in the integral $p \gtrsim T$, the production and relaxation rates only differ by a few percent, and the results for the relaxation rates yield a reliable approximation to the production rate.

An important bonus of obtaining the production rate from the quasiparticle decay width as carried out here is

the correct dependence on the mixing angle in the medium, which would be missed by a naive perturbative calculation.

Therefore the quasiparticle width yields an excellent approximation to the production rate, in particular, it describes correctly the dependence on the mixing angles in the medium, its magnitude, and k-dependence.

In particular, the result (5.23) confirms the result of Ref. [43] for $Y_1 = 0$. For the scalar contribution bsm the right- and left-handed yield the same result [multiplying (5.23) by a factor 2 in the total rate] and as discussed above the production rate is twice the width, which restores the factor 4 between (5.23) and the result in Ref. [43] which corresponds to the case $Y_1 = 0$.

Thus we conclude that the results of Eqs. (5.4), (5.5), (5.7), (5.8), (5.11), and (5.12) along with the explicit forms (5.22), (5.23), (5.24), and (5.25) provide a complete and reliable assessment of the production rates ready to be input in the kinetic equations that include the cosmological expansion [43].

C. Weak or strong damping?

We have now all the ingredients to assess under which circumstances the weak ($|\tilde{\gamma}| \ll 1$) or strong ($|\tilde{\gamma}| \gg 1$) damping conditions are fulfilled. In terms of the widths and real parts it follows that

$$
\tilde{\gamma} \simeq \frac{2k}{M_s^2} \frac{[\Gamma_{aa}(k) - \Gamma_{ss}(k)]}{[(\cos(2\theta) + \Delta_R(k))^2 + \sin^2(2\theta)]^{1/2}}. \quad (5.33)
$$

For $h = -1$, $\Gamma_{aa} - \Gamma_{ss}$, and Δ_R are dominated by the sm contributions, therefore from Eqs. (4.13) and (5.24) we find

$$
\Delta_R(k) \sim \frac{g^2}{16\pi^2} \frac{kT}{M_s^2} \mathcal{A}(k), \qquad (5.34)
$$

$$
\Delta_I(k) \sim \frac{g^2}{32\pi} \frac{kT}{M_s^2} \left(\frac{M_Z}{k}\right)^2 \mathcal{B}(k), \qquad (5.35)
$$

where $\mathcal{A}(k)$, $\mathcal{B}(k)$ can be read off (4.13) and (5.24). In the region of parameters where $\Delta_R(k) \gg \cos(2\theta) \sim 1$, it follows that $\tilde{\gamma} \simeq \Delta_I(k)/\Delta_R(k)$; furthermore, for $k < T \sim M_{Z,W}$ the function $\mathcal{B}(k) \sim e^{-x_Z^*} \ll 1$, leading to $\Delta_I/\Delta_R \ll 1$ corresponding to the weak damping case in which the widths (production rates) are given by (5.7) and (5.8).

Far away from the MSW resonances but in the region where $\cos(2\theta) \sim 1 \gg \Delta_R(k)$ it also follows that $\Delta_I/\Delta_R \ll 1$, corresponding again to the weak damping regime. Therefore the parameter region *far away* from MSW resonances (either above or below) corresponds to the weak damping regime.

Very near MSW resonances $\cos(2\theta) + \Delta_R \sim 0$ and $\tilde{\gamma} \sim \Delta_I/|\sin(2\theta)|$, in the region of relevance for our analysis $T \sim M_{Z,W}$ with $M_s \sim$ KeV it follows that

$$\frac{\Delta_I(k)}{|\sin(2\theta)|} \sim \frac{4 \times 10^{13}}{|\sin(2\theta)|} \left(\frac{k}{T}\right) \left(\frac{M_Z}{k}\right)^2 \mathcal{B}(k), \quad (5.36)$$

therefore, since the resonance occurs at $k/T < 1$ for $M_{Z,W} \sim T$ we conclude that the strong damping condition $\tilde{\gamma} \gg 1$ is fulfilled *near MSW resonances*. Because the MSW resonance(s) are very narrow for $T \simeq M_{Z,W}$ as discussed above [see the discussion leading to Eq. (4.16)], we conclude that in *most* of the regime of temperatures and momenta the weak damping results (5.7) and (5.8) are valid and only in a very narrow region near MSW resonances the strong damping results (5.11) and (5.12) are valid.

An identical analysis confirms a similar conclusion for the case $h = 1$, namely, the weak damping condition holds in most of the relevant range of M/T; k/T but for a narrow region near the MSW resonances in which the strong damping condition holds.

An alternative interpretation of the weak and strong damping regime is obtained using Eq. (5.9) to write

$$\tilde{\gamma} \simeq \frac{\Gamma_{aa} - \Gamma_{ss}}{\Delta\Omega_{\text{wd}}}. \quad (5.37)$$

Since $\Delta\Omega_{\text{sd}} \leq \Delta\Omega_{\text{wd}}$ the denominator gives an upper bound to the *oscillation frequency* between the active and sterile neutrinos. The weak damping regime $|\tilde{\gamma}| \ll 1$ describes the case in which there are many oscillations before the overlap amplitude is suppressed, whereas the strong damping regime describes the case in which damping occurs before oscillations take place. For a similar discussion see the second reference in [56].

D. Regime of validity of perturbation theory

In the relativistic approximation the validity of the perturbative expansion requires that $k \gg \Sigma_{\text{bsm}}$; Σ_{sm}. Since the weak interaction coupling constant g_{sm} is much larger than $Y_{1,2}$ we focus on the standard model contributions.

From the expression (4.8) and the results displayed in Fig. 7 we see that for $M_W/T \gtrsim 1$, it follows that $\text{Re}\Sigma_{\text{sm}} \propto \alpha_w T$ since the coefficient functions A, $B \lesssim 12$. Therefore perturbation theory is valid for $k \gg T/30$, hence for $M_W/T \gtrsim 1$ the resonances in absence of lepton asymmetry at $0.2 \lesssim k/T \lesssim 1$ for $1 \lesssim M_W/T \lesssim 3$ are comfortably within the regime of validity of the perturbative expansion. The lepton-asymmetry induced resonance for $k/T \ll M_W/T$ is the usual resonance and for $T \ll M_W$ the expressions (4.9), (4.10), and (4.11) reduce to the results available in the literature [53,54]. In the regime $k \ll T < M_W$ the on-shell self-energies are linear in k. We see that, for $g^2 \sim 0.4$, the terms proportional to k are $\ll 1$ for $M_W \gtrsim 2T$, hence perturbation theory is reliable within the regime of interest in this article. The imaginary parts are always perturbatively small because of the exponential suppression factors $e^{-M^2/kT}$.

Perturbation theory breaks down for $M \lesssim T$ for the small k/T region and requires a hard thermal loop resum-

mation program [62] akin to the one presented in Ref. [57] in the standard model without mixing. This is well known in gauge theories where the gauge bosons are nearly massless on the scale T [62]. Such a program is well beyond the realm of this study, however, for $M/T \gtrsim 1$–3 our results are reliable for $k/T \gg \alpha_w$ as analyzed above. For example for the case $M/T \sim 1$ although the peak in the coefficients A, B in the self-energy occur for $k/T \approx 0.07$ which is not too large compared to $\alpha_w \sim 0.03$, the position of the resonance at $k/T \sim 0.2$ is well within the regime of validity of the perturbative expansion. The validity of perturbation theory improves dramatically for $M/T > 1$ even in the low momentum region as discussed above. Therefore, we conclude that for $M/T > 1$ the perturbative results are reliable for $k/T > \alpha_w$, in particular, the new resonances are well within the regime of validity of the perturbative expansion. The results for the production rates are always perturbatively small and reliable because of the exponential suppression factor.

VI. DISCUSSION

Our goal is to study the production of sterile neutrinos in cosmology near the electroweak scale when the universe is radiation dominated. To include the effects of cosmological expansion in the production rates and mixing angles, one must first replace the momentum $k \rightarrow k_p(t) = k/a(t)$ and temperature $T \rightarrow T(t) = T_i a_i/a(t)$ where k is the comoving momentum, $a(t)$ the scale factor, and T_i; a_i correspond to the initial temperature and scale factor at which the kinetic equations are initialized. Whereas the ratio $k_p(t)/T(t) = k/(T_i a_i)$ is constant $M/T(t) = Ma(t)/(T_i a_i)$ *grows* during the expansion. Consider setting initial conditions at $T_i \lesssim M_W$, so that $M/T_i \sim 1$, the analysis of Sec. IV shows that there exists at least one very narrow MSW resonance even for *nearly right-handed sterile neutrinos* (two if a lepton asymmetry in the neutrino sector is included) at a value $(k_p(t)/T(t))_c < 1$. For $(k_p(t)/T(t)) < (k_p(t)/T(t))_c$ the analysis shows that $\Delta_R \gg 1$ and

$$\theta_m \sim \frac{\theta}{\Delta_R} \ll \theta, \quad (6.1)$$

therefore for $(k_p(t)/T(t)) < (k_p(t)/T(t))_c$ we find

$$\Gamma_1 \sim \Gamma_{aa}, \qquad \Gamma_2 \sim \Gamma_{ss} + \left(\frac{\theta}{\Delta_R}\right)^2 \Gamma_{aa}. \quad (6.2)$$

For these values of $k_p(t)/T(t)$ the mode "1" is activelike and it is produced with a weak interaction rate, whereas the mode "2" is sterilelike and is produced with the rate similar to that of Ref. [43] plus small corrections from standard model interaction rates suppressed by the mixing angle in the medium $\sim\theta/\Delta_R$. On the other hand for $(k_p(t)/T(t)) > (k_p(t)/T(t))_c$ we found above that $\Delta_R \ll -1$ leading to $\theta_m \sim \pi/2$, namely, the mode "1" is sterilelike and the mode "2" is activelike, with the production

rates

$$\Gamma_1 \sim \left(\frac{\theta}{2\Delta_R}\right)^2 \Gamma_{aa} + \Gamma_{ss}, \qquad \Gamma_2 \sim \Gamma_{aa}. \qquad (6.3)$$

As the cosmological expansion proceeds eventually $M/T(t) \gg 1$ and the resonances disappear (in absence of lepton asymmetry the MSW resonances for $k_p(t)/T(t) < 1$ disappear for $M/T(t) \gtrsim 3$), Δ_R remains large but positive and the mixing angle in the medium is given by (6.1) and the production rates are given by (6.2) for all values of $k_p(t)/T(t)$, namely, the mode "1" remains the activelike and the mode "2" the sterilelike.

We note that (see Sec. VA)

$$\Gamma_{ss}, \qquad \Gamma_{aa} \propto \left(\frac{M^2}{k^2}\right) \ln\left[\frac{1}{1 - e^{-x^*}e^{-y}}\right], \qquad (6.4)$$

this is precisely the form of the production rate that leads to a distribution function after freeze-out that is enhanced at small momentum, a feature that leads to a larger free-streaming length and transfer function at small scales [43].

During the time when $M/T(t) \sim 1$ the MSW resonance for $k_p(t)/T(t) < 1$ leads to a *nonthermal* population of neutrinos: for $(k_p(t)/T(t)) < (k_p(t)/T(t))_c$ there is a large production of mode "1" leading to large populations and a small production of "2" (sterilelike) leading to small populations, whereas for $(k_p(t)/T(t)) > (k_p(t)/T(t))_c$ there is a "population inversion" in the sense that mode "1" is slightly populated whereas mode "2" will be substantially populated, however, without the small momentum enhancement. Consider a fixed value of $k_p(t)/T(t) < 1$ during the cosmological expansion the ratio $M/T(t) \propto a(t)$ increases sweeping through the MSW resonance, when this happens the mixing angle in the medium vanishes very rapidly because the resonance is very narrow and the mode "2" becomes sterilelike. As the expansion continues the MSW resonances (in absence of lepton asymmetry) disappear altogether and the mixing angles and production rates are given by (6.1) and (6.2), respectively, for *all values* of $k_p(t)/T(t)$. The population of the activelike neutrino (mode "1") continues to build up via weak interaction processes, including those that become dominant at $T \ll M_W$ and eventually thermalizes, whereas the population of the sterilelike neutrino will be frozen out as the production rate Γ_2 shuts off as Γ_{ss} vanishes rapidly for $M/T(t) \ll 1$ (see Ref. [43]) and $\theta_m \rightarrow 0$ as $M/T(t) \gg 1$ even when Γ_{aa} (weak interaction rates) remain large down to the decoupling temperature of weak interactions ~ 1 MeV.

This analysis indicates that sterile neutrino production via the decay of scalar or vector bosons will be effective only in a region for $M_W/T(t) \sim 1$ and the distribution function at freeze-out will be *strongly nonthermal* with very small population but with an enhancement at small momentum as found in Ref. [43]. However, the weak interaction contribution will freeze out much later, depend-ing on the temperature dependence of the mixing angle in the medium and will eventually merge with the nonreso-nant DW production mechanism [27] at $T \sim 150$ MeV.

However the nonthermal distribution built up during the stage when scalar and vector boson decay dominate the production will remain.

At this stage it is important to understand the self-consistency of the analysis. In obtaining the self-energies we had assumed that the eigenstate "1" is activelike with a thermal distribution function. We have learned, however, that there are resonances and the eigenstates "1" and "2" are either activelike or sterilelike depending on k, namely, on which side of the MSW resonance the wave vector lies. This finding calls into question the thermal nature of the neutrino propagator in the intermediate state (of course there is no such ambiguity in the charged lepton propagator that enters in the charged current self-energy). This issue notwithstanding, we have found that the fermionic and bosonic contributions to the real parts of the self-energies are *qualitatively the same* with a rather small quantitative difference, both for sm and bsm contributions. Therefore replacing the thermal fermion propagator for a vacuum one leads to a minor quantitative modification of our argu-ments. However because of the enormous prefactors the conclusions about the sharpness of the resonance and the resonance positions *do not change* and the general analysis remains the same. Therefore, we conclude that the results obtained above are very *robust* not depending on whether the intermediate fermion line features a thermal or vacuum propagator or nonthermal propagator interpolating be-tween these two cases.

VII. CONCLUSIONS AND COSMOLOGICAL CONSEQUENCES

A comprehensive program to assess the viability of any potential DM candidate begins with the microphysics of the production and freeze-out process of the particle phys-ics candidate. This initial step determines the distribution function at freeze-out which in turn determines, along with the mass, its abundance, free-streaming length, phase space density at decoupling, and the transfer function and power spectrum in the linear regime. Our objective is to carry out this program for sterile neutrinos with mass in the KeV range which seems to be the range favored not only as a DM candidate but also provide potential solutions to a host of astrophysical problems [31].

In this article we focus on the first step of the program and study the production of sterile neutrinos in a tempera-ture regime near the electroweak scale in an extension beyond the standard model in which the seesaw mass matrix emerges from expectation values of Higgslike sca-lars with masses of the order of the electroweak scale. This simple and compelling extension which features only one scale yields rich phenomenology [30–32]. The main ob-servation in this article is that in this temperature range

sterile neutrinos are produced by the decay not only of the Higgslike scalar as explored in Refs. [32,43] but also of the *charged and neutral vector bosons* of the standard model. We consider active and sterile species to be Dirac fermions to allow the possibility to include a lepton asymmetry hidden in the (active) neutrino sector consistent with recent bounds from WMAP and BBN [60].

The assessment of the contribution from standard model vertices to sterile neutrino production requires an analysis of the mixing angles in the medium and production rates. We obtain both from the study of the full equation of motion of the active and sterile neutrinos that input the self-energies in the medium. The real part of the self-energy (index of refraction) determines the dispersion relations and mixing angles in the medium, and the imaginary (absorptive) part determines the production rates.

We provide a detailed analysis of the contributions from "beyond the standard model" and standard model interactions to the mixing angles, dispersion relations, and production rates, thereby facilitating the analysis of different situations. The study of the "index of refraction" in the temperature regime near the electroweak scale has not been performed before and yields a wealth of remarkable phenomena.

Our study reveals the presence of narrow MSW resonances *even in the absence of a lepton asymmetry*, in the temperature regime $T \gtrsim M_W$ for $k/T \lesssim 1$. For vanishing lepton asymmetry the resonance occurs at a value $(k/T)_c$ that depends on the ratio M_W/T with $0.15 \lesssim (k/T)_c \lesssim 1$ for $1 \lesssim (M_W/T) \lesssim 3$. The position of the resonance $(k/T)_c$ increases with M_W/T, the resonance eventually disappears for $M_W \gg T$ recovering the result valid in the Fermi limit of the weak interactions [53,54].

Including the possibility of a (small) lepton asymmetry in the neutrino sector with a value compatible with the bounds from WMAP and BBN [60] yields *two* narrow MSW resonances in these regions, with the resonance associated with the lepton asymmetry occurring at $k < \mu \ll T$ where μ is the chemical potential for the active species that determines the lepton asymmetry.

A remarkable aspect of these results is that near these resonances the contribution of the imaginary part of the self-energies leads to a strong damping regime, and the difference in the propagating frequencies *vanishes* exactly at the position of the resonance, with a concomitant breakdown of adiabaticity. For $M_W \gg T$ the MSW resonances that are independent of the lepton asymmetry disappear leaving only the low energy resonances associated with the lepton asymmetry.

Furthermore, we have found that it is quite possible that the region of parameters of the extension bsm allow for MSW resonance for positive energy, positive helicity, namely, nearly *right-handed* states both with and without lepton asymmetry. We also find that the decay of the Z^0, $W^\pm$ vector bosons leads to the production of nearly *right-handed* sterilelike neutrinos.

Because the resonances are very narrow, we obtain a simple expression for the production rates (see Sec. VI) that is valid in a wide range of temperatures and clearly displays the contribution from standard model and beyond standard model interactions.

We have argued that in the early universe the cosmological expansion leads to a highly *nonthermal* distribution function for sterile neutrinos with an enhancement of the low momentum region $k < T$ both as a consequence of the MSW resonances and the vanishing of the mixing angle and production rates as the temperature falls well below the electroweak scale. Furthermore, we expect that because the MSW resonances are very narrow, the cosmological expansion will lead to sterile neutrino production resulting in a highly nonthermal distribution with low momentum enhancement. The form of the production rates via scalar and vector boson decay are similar to that in Ref. [43], which leads us to conjecture that the distribution function after freeze-out will be enhanced in the low momentum region, leading to a smaller free-streaming length and larger power spectrum at small scales as compared to the DW mechanism [27,43].

The next step of the program will input these results into the kinetic equations that describe the production and freeze-out of the sterile species from which the distribution function at decoupling is obtained. We expect to report on these studies in a forthcoming article.

An important remaining question is the extrapolation of these results to $T \gg M_{W,Z}$. At temperatures above the electroweak symmetry breaking scale the $SU(2) \times U(1)$ symmetry is restored and the vector bosons become massless at tree level, therefore the production channel described here shuts off. However, vector bosons acquire electric screening masses of order gT [62] and scalar bosons may also acquire thermal mass corrections of $\mathcal{O}(Y_{1,2}T)$.

Furthermore the seesaw mass matrix also vanishes at tree level if all the mass terms arise from the expectation value of the Higgslike scalar field. This high temperature regime requires a deeper understanding of radiative corrections to the propagators of the vector bosons, in particular, the hard-thermal loop corrections [62].

Understanding the possibility of sterile neutrino production in this high temperature regime entails a nonperturbative resummation program also for neutrinos, akin to the study in Ref. [57]. This program although clearly interesting in its own right is far beyond the realm of our goals here and deserves a deeper study.

Croucher Foundation and Berkeley Center for Theoretical Physics.

APPENDIX A: VECTOR BOSON EXCHANGE SM

The SM self-energy contributions with the exchange of a vector boson are given by the spectral representation (3.5) with the imaginary part given by Eq. (3.14) which is of the form

$$\text{Im}\Sigma_{\text{sm}}(\omega, \vec{k}) = \frac{\pi g_{\text{sm}}^2}{4} \int \frac{d^3 p}{(2\pi)^3 p W_{\vec{p}+\vec{k}}} [\gamma^0 \Pi_{\text{sm}}^0(\omega, \vec{p}, \vec{k})$$

$$- \vec{\gamma} \cdot \hat{k} \Pi_{\text{sm}}^1(\omega, \vec{p}, \vec{k})]. \tag{A1}$$

Neglecting the mass of the neutrinos and charged leptons we find

$$\Pi_{\text{sm}}^0(\omega, \vec{p}, \vec{k}) = [1 - n_F(p) + N_B(W_{\vec{p}+\vec{k}})]\left[p\left(1 + \frac{2W_{\vec{p}+\vec{k}}^2}{M^2}\right) + \frac{2W_{\vec{p}+\vec{k}}}{M^2}(p^2 + \vec{k} \cdot \vec{p})\right]\delta(\omega - p - W_{\vec{p}+\vec{k}})$$

$$+ [1 - \bar{n}_F(p) + N_B(W_{\vec{p}+\vec{k}})]\left[p\left(1 + \frac{2W_{\vec{p}+\vec{k}}^2}{M^2}\right) + \frac{2W_{\vec{p}+\vec{k}}}{M^2}(p^2 + \vec{k} \cdot \vec{p})\right]\delta(\omega + p + W_{\vec{p}+\vec{k}})$$

$$+ [n_F(p) + N_B(W_{\vec{p}+\vec{k}})]\left[p\left(1 + \frac{2W_{\vec{p}+\vec{k}}^2}{M^2}\right) - \frac{2W_{\vec{p}+\vec{k}}}{M^2}(p^2 + \vec{k} \cdot \vec{p})\right]\delta(\omega - p + W_{\vec{p}+\vec{k}})$$

$$+ [\bar{n}_F(p) + N_B(W_{\vec{p}+\vec{k}})]\left[p\left(1 + \frac{2W_{\vec{p}+\vec{k}}^2}{M^2}\right) - \frac{2W_{\vec{p}+\vec{k}}}{M^2}(p^2 + \vec{k} \cdot \vec{p})\right]\delta(\omega + p - W_{\vec{p}+\vec{k}}) \tag{A2}$$

and

$$\Pi_{\text{sm}}^1(\omega, \vec{p}, \vec{k}) = [1 - n_F(p) + N_B(W_{\vec{p}+\vec{k}})]\left[-\hat{k} \cdot \vec{p} + \frac{2(k + \hat{k} \cdot \vec{p})}{M^2}(pW_{\vec{p}+\vec{k}} + p^2 + \vec{k} \cdot \vec{p})\right]\delta(\omega - p - W_{\vec{p}+\vec{k}})$$

$$- [1 - \bar{n}_F(p) + N_B(W_{\vec{p}+\vec{k}})]\left[-\hat{k} \cdot \vec{p} + \frac{2(k + \hat{k} \cdot \vec{p})}{M^2}(pW_{\vec{p}+\vec{k}} + p^2 + \vec{k} \cdot \vec{p})\right]\delta(\omega + p + W_{\vec{p}+\vec{k}})$$

$$+ [n_F(p) + N_B(W_{\vec{p}+\vec{k}})]\left[-\hat{k} \cdot \vec{p} + \frac{2(k + \hat{k} \cdot \vec{p})}{M^2}(-pW_{\vec{p}+\vec{k}} + p^2 + \vec{k} \cdot \vec{p})\right]\delta(\omega - p + W_{\vec{p}+\vec{k}})$$

$$- [\bar{n}_F(p) + N_B(W_{\vec{p}+\vec{k}})]\left[-\hat{k} \cdot \vec{p} + \frac{2(k + \hat{k} \cdot \vec{p})}{M^2}(-pW_{\vec{p}+\vec{k}} + p^2 + \vec{k} \cdot \vec{p})\right]\delta(\omega + p - W_{\vec{p}+\vec{k}}). \tag{A3}$$

APPENDIX B: SCALAR EXCHANGE BSM

For scalar boson exchange we find

$$\text{Im} \Sigma_{\text{bsm}}(\omega, \vec{k}) = \frac{\pi Y^2}{4} \int \frac{d^3 p}{(2\pi)^3 W_{\vec{p}+\vec{k}}} [\gamma^0 \Pi_{\text{bsm}}^0(\omega, \vec{p}, \vec{k}) - \vec{\gamma} \cdot \hat{k}(\hat{k} \cdot \hat{p})\Pi_{\text{bsm}}^1(\omega, \vec{p}, \vec{k})], \tag{B1}$$

where

$$\Pi_{\text{bsm}}^0(\omega, \vec{p}, \vec{k}) = [1 - n_F(p) + N_B(W_{\vec{p}+\vec{k}})]\delta(\omega - p - W_{\vec{p}+\vec{k}}) + [1 - \bar{n}_F(p) + N_B(W_{\vec{p}+\vec{k}})]\delta(\omega + p + W_{\vec{p}+\vec{k}})$$

$$+ [n_F(p) + N_B(W_{\vec{p}+\vec{k}})]\delta(\omega - p + W_{\vec{p}+\vec{k}}) + [\bar{n}_F(p) + N_B(W_{\vec{p}+\vec{k}})]\delta(\omega + p - W_{\vec{p}+\vec{k}}), \tag{B2}$$

$$\Pi_{\text{bsm}}^1(\omega, \vec{p}, \vec{k}) = [1 - n_F(p) + N_B(W_{\vec{p}+\vec{k}})]\delta(\omega - p - W_{\vec{p}+\vec{k}}) - [1 - \bar{n}_F(p) + N_B(W_{\vec{p}+\vec{k}})]\delta(\omega + p + W_{\vec{p}+\vec{k}})$$

$$+ [n_F(p) + N_B(W_{\vec{p}+\vec{k}})]\delta(\omega - p + W_{\vec{p}+\vec{k}}) - [\bar{n}_F(p) + N_B(W_{\vec{p}+\vec{k}})]\delta(\omega + p - W_{\vec{p}+\vec{k}}). \tag{B3}$$

[1] See, for example, J. Primack, New Astron. Rev. **49**, 25 (2005); in *Formation of Structure in the Universe*, edited by A. Dekel and J. P. Ostriker (Cambridge Univ. Press, Cambridge, 1999) and references therein.

[2] A. Klypin *et al.*, Astrophys. J. **522**, 82 (1999); **523**, 32 (1999).

[3] B. Moore *et al.*, Astrophys. J. Lett. **524**, L19 (1999).

[4] G. Kauffman, S. D. M. White, and B. Guiderdoni, Mon. Not. R. Astron. Soc. **264**, 201 (1993).

[5] S. Ghigna *et al.*, Astrophys. J. **544**, 616 (2000).

[6] J. Diemand *et al.*, Astrophys. J. **657**, 262 (2007); **667**, 859 (2007).

[7] M. Kuhlen *et al.*, J. Phys. Conf. Ser. **125** 012008 (2008).

[8] J. F. Navarro, C. S. Frenk, and S. White, Mon. Not. R. Astron. Soc. **462**, 563 (1996).

[9] J. Dubinski and R. Carlberg, Astrophys. J. **378**, 496 (1991).

[10] J. S. Bullock *et al.*, Mon. Not. R. Astron. Soc. **321**, 559 (2001); A. R. Zentner and J. S. Bullock, Phys. Rev. D **66**, 043003 (2002); Astrophys. J. **598**, 49 (2003).

[11] J. Diemand *et al.*, Mon. Not. R. Astron. Soc. **364**, 665 (2005).

[12] J. T. Kleyna *et al.*, Mon. Not. R. Astron. Soc. **330**, 792 (2002).

[13] J. J. Dalcanton and C. J. Hogan, Astrophys. J. **561**, 35 (2001).

[14] R. F. G. Wyse and G. Gilmore, arXiv:0708.1492; G. Gilmore *et al.*, Astrophys. J. **663** 948 (2007); arXiv:0804.1919; arXiv:astro-ph/0703370; G. Gilmore *et al.*, Nucl. Phys. B, Proc. Suppl. **173**, 15 (2007).

[15] G. Gentile *et al.*, Astrophys. J. Lett. **634**, L145 (2005); Mon. Not. R. Astron. Soc. **351**, 903 (2004); V. G. J. De Blok *et al.*, Mon. Not. R. Astron. Soc. **340**, 657 (2003); G. Gentile *et al.*, Astron. Astrophys. **467** 925 (2007).P. Salucci and A. Sinibaldi, Astron. Astrophys. **323**, 1 (1997); G. Gentile *et al.*, Astron. Astrophys. **467**, 925 (2007).

[16] S. S. McGaugh *et al.*, Astrophys. J. **659**, 149 (2007).

[17] G. Battaglia *et al.*, arXiv:0802.4220.

[18] N. W. Evans *et al.*, arXiv:0811.1488.

[19] A. Tikhonov and A. Klypin, arXiv:0807.0924.

[20] B. Moore *et al.*, Mon. Not. R. Astron. Soc. **310**, 1147 (1999).

[21] P. Bode, J. P. Ostriker, and N. Turok, Astrophys. J. **556**, 93 (2001).

[22] V. Avila-Reese *et al.*, Astrophys. J. **559**, 516 (2001).

[23] A. Knebe *et al.*, Mon. Not. R. Astron. Soc. **329**, 813 (2002); **345**, 1285 (2003).

[24] J. R. Bond, G. Efstathiou, and J. Silk, Phys. Rev. Lett. **45**, 1980 (1980).

[25] M. K. R. Joung, R. Cen, and G. Bryan, Astrophys. J. Lett. **692** L1 (2009).

[26] A. Knebe *et al.*, arXiv:0802.1628; B. Arnold *et al.*, arXiv:0811.1851.

[27] S. Dodelson and L. M. Widrow, Phys. Rev. Lett. **72**, 17 (1994).

[28] S. Colombi, S. Dodelson, and L. M. Widrow, Astrophys. J. **458**, 1 (1996).

[29] X. Shi and G. M. Fuller, Phys. Rev. Lett. **82**, 2832 (1999); K. Abazajian, G. M. Fuller, and M. Patel, Phys. Rev. D **64**, 023501 (2001); K. Abazajian and G. M. Fuller, Phys. Rev.

D **66**, 023526 (2002); G. M. Fuller *et al.*, Phys. Rev. D **68**, 103002 (2003); K. Abazajian, Phys. Rev. D **73**, 063506 (2006).

[30] M. Shaposhnikov and I. Tkachev, Phys. Lett. B **639**, 414 (2006); M. Shaposhnikov, J. High Energy Phys. 08 (2008) 008; J. High Energy Phys. 08 (2008) 008.

[31] A. Kusenko, arXiv:hep-ph/0703116; Int. J. Mod. Phys. D **16** 2325 (2007); T. Asaka, M. Shaposhnikov, and A. Kusenko, Phys. Lett. B **638**, 401 (2006); P. L. Biermann and A. Kusenko, Phys. Rev. Lett. **96**, 091301 (2006).

[32] K. Petraki and A. Kusenko, Phys. Rev. D **77**, 065014 (2008).

[33] K. Petraki, Phys. Rev. D **77**, 105004 (2008).

[34] D. Boyanovsky, H. J. de Vega, and N. Sanchez, Phys. Rev. D **77**, 043518 (2008).

[35] A. Boyarsky, O. Ruchayskiy, and M. Shaposhnikov, arXiv:0901.0011.

[36] C. J. Hogan and J. J. Dalcanton, Phys. Rev. D **62**, 063511 (2000).

[37] A. Boyarsky *et al.*, Mon. Not. R. Astron. Soc. **370**, 213 (2006); Phys. Rev. D **74**, 103506 (2006); AAS Sci. Technol. Ser. **471**, 51 (2007); Astropart. Phys. **28**, 303 (2007); C. R. Watson *et al.*, Phys. Rev. D **74**, 033009 (2006).

[38] U. Seljak *et al.*, Phys. Rev. Lett. **97**, 191303 (2006); M. Viel *et al.*, Phys. Rev. Lett. **97**, 071301 (2006).

[39] M. Viel *et al.*, Phys. Rev. Lett. **100**, 041304 (2008); A. Boyarski *et al.*, arXiv:0812.0010.

[40] A. Palazzo *et al.*, arXiv:0707-1495.

[41] T. Asaka, M. Laine, and M. Shaposhnikov, J. High Energy Phys. 01 (2007) 091; 06 (2006) 053; T. Asaka and M. Shaposhnikov, Phys. Lett. B **620**, 17 (2005); T. Asaka, S. Blanchet, and M. Shaposhnikov, Phys. Lett. B **631**, 151 (2005).

[42] A. Kusenko, Phys. Rev. Lett. **97**, 241301 (2006).

[43] D. Boyanovsky, Phys. Rev. D **78**, 103505 (2008).

[44] D. Boyanovsky, H. J. de Vega, and N. Sanchez, Phys. Rev. D **78**, 063546 (2008).

[45] D. Boyanovsky, Phys. Rev. D **77**, 023528 (2008).

[46] H. J. de Vega and N. G. Sanchez, arXiv:0901.0922.

[47] A. Boyarski, J. Lesgourgues, O. Ruchayskiy, and M. Viel, Phys. Rev. Lett. **102**, 201304 (2009).

[48] M. Loewenstein, A. Kusenko, and P. L. Biermann, Astrophys. J. **700**, 426 (2009).

[49] L. Wolfenstein, Phys. Rev. D **17**, 2369 (1978); S. P. Mikheyev and A. Yu. Smirnov, Sov. J. Nucl. Phys. **42**, 913 (1985).

[50] C. W. Kim and A. Pevsner, *Neutrinos in Physics and Astrophysics* (Harwood Academic Publishers, Chur, Switzerland, 1993).

[51] R. N. Mohapatra and P. B. Pal, *Massive Neutrinos in Physics and Astrophysics* (World Scientific, Singapore, 2004).

[52] M. Fukugita and T. Yanagida, *Physics of Neutrinos and Applications to Astrophysics* (Springer-Verlag, Berlin Heidelberg, 2003).

[53] D. Notzold and G. Raffelt, Nucl. Phys. **B307**, 924 (1988).

[54] C. M. Ho, D. Boyanovsky, and H. J. de Vega, Phys. Rev. D **72**, 085016 (2005).

[55] A. D. Dolgov, Surveys High Energ. Phys. **17**, 91 (2002); Phys. Rep. **370**, 333 (2002).

[56] C. M. Ho and D. Boyanovsky, Phys. Rev. D **73**, 125014 (2006); D. Boyanovsky and C. M. Ho, J. High Energy Phys. 07 (2007) 030; Astropart. Phys. **27**, 99 (2007).

[57] D. Boyanovsky, Phys. Rev. D **72**, 033004 (2005).

[58] D. Boyanovsky, K. Davey, and C. M. Ho, Phys. Rev. D **71**, 023523 (2005).

[59] S. Y.-Wang, D. Boyanovsky, H. J. de Vega, D.-S. Lee, and Y. J. Ng, Phys. Rev. D **61**, 065004 (2000); D. Boyanovsky, H. J. de Vega, D.-S. Lee, Y. J. Ng, and S.-Y. Wang, Phys. Rev. D **59**, 105001 (1999), and references therein.

[60] V. Simha and G. Steigman, J. Cosmol. Astropart. Phys. 08 (2008) 011.

[61] A. de Gouvea, arXiv:0706.1732; A. de Gouvea, J. Jenkins, and N. Vasudevan, Phys. Rev. D **75**, 013003 (2007).

[62] R. D. Pisarski, Phys. Rev. Lett. **63**, 1129 (1989); Physica A (Amsterdam) **158**, 246 (1989); Nucl. Phys. **B309**, 476 (1988); E. Braaten and R. Pisarski, Nucl. Phys. **B337**, 569 (1990); **B339**, 310 (1990); J. Frenkel and J. C. Taylor, Nucl. Phys. **B334**, 199 (1990).

[63] D. Boyanovsky, Phys. Rev. D **76**, 103514 (2007).